



Published in final edited form as:

J Med Chem. 2013 August 8; 56(15): 6216–6233. doi:10.1021/jm400664x.

Heteroaromatic and aniline derivatives of piperidines as potent ligands for vesicular acetylcholine transporter

Junfeng Li^a, Xiang Zhang^a, Zhanbin Zhang^a, Prashanth K. Padakanti^a, Hongjun Jin^a, Jinquan Cui^a, Aixiao Li^a, Dexing Zeng^a, Nigam P. Rath^b, Hubert Flores^c, Joel S. Perlmutter^{a,c}, Stanley M. Parsons^d, and Zhude Tu^{a,*}

^aDepartment of Radiology, Washington University School of Medicine, 510 S. Kingshighway Blvd, St. Louis, MO 63110

^bDepartment of Chemistry and Biochemistry and Center for Nanoscience, University of Missouri - St. Louis, One University Boulevard, St. Louis, MO 63121

^cDepartment of Neurology, Washington University School of Medicine, 660 South Euclid, St. Louis, MO 63110

^dDepartment of Chemistry and Biochemistry and the Graduate Program in Biomolecular Science and Engineering, University of California, Santa Barbara, CA 93106

Abstract

To identify suitable lipophilic compounds having high potency and selectivity for vesicular acetylcholine transporter (VACHT), a heteroaromatic ring or a phenyl group was introduced into the carbonyl-containing scaffold for VACHT ligands. Twenty new compounds with ALog D values between 0.53–3.2 were synthesized, and their *in vitro* binding affinities were assayed. Six of them (**19a**, **19e**, **19g**, **19k** and **24a-b**) displayed high affinity for VACHT ($K_i = 0.93 - 18$ nM for racemates) and moderate to high selectivity for VACHT over α_1 and α_2 receptors ($K_i = 44 - 4400$ -fold). These compounds have a methyl or a fluoro substitution that provides the position for incorporating PET radioisotopes C-11 or F-18. Compound (-)-[¹¹C]**24b** ($K_i = 0.78$ for VACHT, 900-fold over α receptors) was successfully synthesized and evaluated *in vivo* in rats and nonhuman primates. The data revealed that (-)-[¹¹C]**24b** has highest binding in striatum and has favorable pharmacokinetics in the brain.

Keywords

Blood-brain-barrier (BBB); lipophilicity; sigma-1 and sigma-2 receptors; structure-activity relationship (SAR); vesicular acetylcholine transporter (VACHT)

Introduction

Dementia is a clinical syndrome characteristic of loss or decline in memory and other cognitive abilities that result in functional impairment in the elderly. It is a global public health problem.^{1, 2} The prevalence in the USA has been recently estimated at 5.4 million individuals, including 5.2 million over the age of 65, and 200,000 individuals under the age

*Address correspondence to: Zhude Tu, Ph.D., Department of Radiology, Washington University School of Medicine, Campus Box 8225, 510 S. Kingshighway Blvd., St. Louis, MO 63110, USA, Tel: 1-314-362-8487, Fax: 1-314-362-8555, tuz@mir.wustl.edu.

Supplementary Material

Supporting Information Available: [Elemental analyses of new analogues and X-ray structural data of **19i**]. This material is available free of charge via the internet at <http://pubs.acs.org>.

of 65.¹ Increasing lifespan of people will lead to increased number of patients with dementia. The severity of dementia in neurodegenerative diseases is linked to loss of cholinergic neurons and synapses in the central nervous system (CNS). The use of ¹¹C-labeled Pittsburgh Compound-B ([¹¹C]PIB) to assess β -amyloid plaques and diagnose Alzheimer's disease (AD) was a significant breakthrough.³ However, [¹¹C]PIB cannot specifically assess the loss of cholinergic neurons and synapses in the brain, which correlates to severity of cognitive dysfunction in AD.⁴⁻⁹ For Parkinson's disease associated with dementia (PDD), the cholinergic deficit in cortical regions is more severe than for non-demented patients with Parkinson's Disease (PD).¹⁰ A PET tracer that can assess the loss of cholinergic synapses would provide a useful tool for assessing the severity of cognitive dysfunction and monitoring the efficacy of cholinergic therapies for dementia in neurodegenerative disorders.

Vesicular acetylcholine transporter (VACHT) and choline acetyltransferase (ChAT) are essential for a cholinergic neuron.¹¹ VACHT is localized in cholinergic terminals, and it transports acetylcholine (ACh) from the cytoplasm into the synaptic vesicles. Anti-ChAT preferentially stains cell bodies, whereas anti-VACHT preferentially stains nerve terminals.^{4, 12} Anti-ChAT is more useful for monitoring the death of cholinergic cells, whereas anti-VACHT is more useful for monitoring changes in the density of cholinergic terminals. It is widely accepted that VACHT is a reliable biomarker to study cholinergic function in the brain. Currently, (-)-5-[¹²³I]iodobenzovesamicol ([¹²³I]IBVM) is the only radiotracer used for imaging VACHT levels in living human brain using single-photon emission computed tomography (SPECT). The relative distribution for specific binding of [¹²³I]IBVM in human brain corresponds well with postmortem results reported for ChAT.^{13, 14} When [¹²³I]IBVM was used to assess cholinergic deficiency in patients with dementia, it was found that PDD and AD patients have globally reduced cortical binding.¹⁵ In addition, a significant decrease in [¹²³I]IBVM binding (47-62%) in cingulate cortex and parahippocampal amygdaloid in AD subjects compared to control patients has been observed.¹⁶ However, the slow binding kinetics of [¹²³I]IBVM requires scanning for approximately 6 hours post-injection, which can be stressful for patients. Positron emission tomography (PET) imaging will be able to carry out scans with higher sensitivity and spatial resolution (3-5 mm) compared to SPECT (10 mm).^{17, 18} The demand to provide higher accuracy in clinical imaging of VACHT levels in humans makes the identification of a PET tracer for VACHT very important. To date, this goal has not been achieved because of the lack of suitable PET radiotracers.

In efforts to develop a PET tracer for VACHT, investigators have put tremendous effort into optimizing the structure of vesamicol analogues with the goal of identifying highly potent and selective ligands.^{4, 19-27} Among various radioligands developed, only a small number have been evaluated *in vivo* in non-human primates and humans.^{19, 27-29} Despite promising *in vitro*, *ex vivo* and initial *in vivo* studies, most of the ligands are unsuitable for clinical use due to poor selectivity over α receptors in brain, low extraction from the blood, slow brain kinetics or fast metabolism. Among the physicochemical properties of ligands, lipophilicity is one of the key properties that plays a pivotal role in absorption, distribution, metabolism, and elimination of ligands.³⁰ For central nervous system drugs, it was found that the blood-brain-barrier (BBB) penetration is optimal with the ALog D values in the range of 1.5 – 3.0, with a mean value of 2.5.³¹⁻³³ Although other properties of compounds affect the BBB penetration, those ligands with moderate lipophilicity often exhibit highest brain uptake.³⁰ Highly lipophilic radiotracers are usually cleared slowly from the brain.

Our group has reported a new class of VACHT inhibitors containing a carbonyl group attached to the 4 position of the piperidine ring and discussed the structure-activity relationship (SAR) of this new class of compounds.^{4, 19, 34-36} Among them (as shown in

Figure 1), compounds **5**, **7** and **8** displayed high potencies and good selectivity for VACHT *in vitro*.^{4, 19} In particular, a fluorine-18 labeled version of (-)-2-hydroxy-3-(4-(4-fluorobenzoyl)piperidino)tetralin, (-)-[¹⁸F]**7** was successfully radiosynthesized and used to conduct *in vivo* evaluation in rats and monkeys; the initial results were very promising.¹⁹ The possibility that (-)-[¹⁸F]**7** can serve as a clinical PET tracer for quantifying the level of VACHT *in vivo* is under investigation. The current manuscript focuses on 1) optimizing the structures of this new class of VACHT ligand to identify highly potent ligands having lipophilicity suitable to efficiently cross the BBB. 2) Separate the enantiomers of the optimal compound, and radiosynthesize with carbon-11 PET isotope. 3) *In vivo* evaluate the new C-11 radiotracer in rodent and non-human primate. The strategies to achieve optimization include: (1) replacing the thiophenyl group in (1-((2S,3S)-3-hydroxy-1,2,3,4-tetrahydronaphthalen-2-yl)piperidin-4-yl)(thiophen-2-yl)methanone **9** with N-methyl pyrrole⁴ (the methyl group provides a position for conveniently labeling with carbon-11 isotope), (2) replacing the 4-fluorophenyl group in **7**⁴ with pyridine, substituted pyridines and pyrroles and optimizing the substitution so that radiolabeling with carbon-11 or fluorine-18 can be achieved, and (3) converting the primary amino group of compound **6** to monomethyl amino or dimethyl amino, which will provide access for radiolabeling with carbon-11. This investigation was inspired by (1) the observation that a series of carbonyl group containing analogues have high affinity for VACHT and low affinity for receptors;^{4, 19, 34} (2) our *in vivo* validation of (-)-[¹⁸F]**7**¹⁹ and its analogue (-)-[¹¹C]**8**,³⁵ which showed high binding in the striatum, the VACHT enriched regions in the brain; and (3) the high demand for a clinically suitable PET probe for investigating the correlation between loss of cognitive function and loss of cholinergic synapses, which will help improve the early diagnosis of dementia and monitor the therapeutic efficacy of treating Alzheimer's and other neurodegenerative diseases.

Results and Discussion

Chemistry

The synthesis of a new series of vesicular acetylcholine transporter inhibitors was accomplished according to Schemes 1-5. *t*-Boc-protected piperidine-4-carboxylic acid (**10**) was treated with 1,1'-carbonyldiimidazole (CDI), and *N,O*-dimethylhydroxylamine to afford Weinreb amide **11**, which served as a versatile intermediate for synthesizing piperidines bearing a substituted heteroaromatic carbonyl group at the 4-position. Bromo substituted heteroaromatic compounds were lithiated with *n*-butyllithium (*n*-BuLi) and reacted with Weinreb amide to afford intermediates **16a-i**. When synthesizing *N*-methyl pyrrole derivative **16a**, via treatment of *N*-methylpyrrole with *n*-BuLi³⁶ followed by compound **11**, it was observed that the yield was much higher if the reaction vessel was pre-cooled to -78 °C while adding *n*-BuLi. To synthesize *N*-methyl pyridine derivatives **16h** and **16i**, commercially available 4 or 6-bromine substituted pyridin-2-amines **12h** and **12i** were first converted to 2-hydroxypyridines **13h** and **13i** or 2-pyridones **14h** and **14i** with sodium nitrite in sulfuric acid^{37, 38} followed by methylation using iodomethane in acetone to form bromo substituted *N*-methyl-2-pyridones **15h** and **15i** as major products.³⁹ These pyridones reacted with **11** to afford the corresponding carbonyl group containing intermediates **16h** and **16i**. Trifluoroacetic acid (TFA) was used to remove the *t*-Boc group in **16a-i** to afford the key intermediates **17a-i**. Treatment of **17a-i** with epoxide 1a,2,7,7a-tetrahydronaphtho[2,3-*b*]oxirene (**18**)⁴ afforded the target compounds **19a-i** as shown in Scheme 1. To confirm whether the methyl group was on the *N*- or *O*-atom of **19h** and **19i**, the X-ray crystal structure of the oxalate salt of **19i** was obtained as shown in Figure 2. The X-ray crystal structure revealed that the methyl group is on the nitrogen.

Although direct condensation of substituted piperidines and epoxide **18** was a common procedure for synthesizing vesicular acetylcholine transporter inhibitors,^{19, 40} it proved challenging when synthesizing **19j** and **19k** due to the low solubility of substituted heteroaromatic piperidines in commonly used solvents such as methanol, ethanol, dichloromethane, DMF and DMSO. Thus, an alternative approach was followed in which the *t*-Boc group in compound **11** was removed first, and the resulting piperidine was treated with **18** to afford compound **20**. The free hydroxyl group of compound **20** was protected with the *tert*-butyldimethylsilyl group by reacting with *tert*-butyldimethylsilyl chloride to afford compound **21**. Commercially available 5-bromo-2-fluoropyridine (**17j**) or 3-bromo-2-fluoropyridine (**17k**) was treated with *n*-BuLi in THF followed by compound **21**, and further removal of TBDMS group afforded target compounds **19j** and **19k** as shown in Scheme 2.

Compounds **24a** and **24b** were synthesized as depicted in Scheme 3. Compound **6** was synthesized following the reported procedure.¹⁹ Direct dimethylation of the aromatic amine in compound **6** with iodomethane in the presence of NaH afforded compound **24a** very easily. However, the synthesis of the *N*-monomethylaniline analogue **24b** was more complicated. The free hydroxyl group and the primary aniline group of **6** were protected by treating with acetic anhydride to form diacetylated compound **22**.⁴¹ *N*-methylation of aromatic amide **22** gave intermediate **23**, which upon hydrolysis afforded the target compound **24b**.

Synthesis of fluoroethoxy analogues **26a** and **26b** followed two different approaches as shown in Scheme 4. The first approach was to demethylate **19e** in the presence of boron tribromide (BBr₃) or trimethylsilyl iodide (TMSI) to generate the corresponding alcohol **25**, which was reacted with 1-bromo-2-fluoroethane to afford the target *O*-alkylated compound **26a**. However, use of a similar approach to synthesize compound **26b** was not successful with either BBr₃ or TMSI to remove the methyl group in **19f**. To overcome this challenge, an alternative approach was used. Commercially available 2-bromopyridin-3-ol (**27**) was reacted with 1-bromo-2-fluoroethane via *O*-alkylation to afford 2-bromo-3-(2-fluoroethoxy)pyridine (**28**). This compound was lithiated and treated with compounds **11**, followed by **18** to afford target compound **26b** following the procedure described for synthesis of compounds **19j** and **19k**.

To make aminobenzovesamicol (ABV) analogues containing substituted heteroaromatic carbonyl groups, namely **30a-d** and **31a**, the corresponding piperidine precursors **17a-d** containing substituted heteroaromatic carbonyl groups were reacted with 2,2,2-trifluoro-*N*-(1a,2,7,7atetrahydronaphtho[2,3-*b*]oxiren-3-yl)acetamide (**29**), which was synthesized by following the literature protocol.⁴ The trifluoroacetyl protection group was then removed via hydrolysis in the presence of sodium hydroxide to afford the regioisomers **30a-d** and **31a** as shown in Scheme 5.

In vitro binding studies revealed that **24b** was highly potent. Therefore, the (-)-**24b** and (+)-**24b** were obtained by separating the enantiomers on HPLC using chiralcel OD column. The precursor (-)-**33** for the radiolabeling of (-)-[¹¹C]**24b** was synthesized as shown in Scheme 6. Briefly, the enantiomeric separation of **6** was performed on chiral HPLC using Chiralcel OD column to give (+)-**6** and (-)-**6**. The (-)-**6** isomer was treated with Boc anhydride in the presence of triethylamine to give the tri-Boc protected intermediate (-)-**32**. 4-Dimethylaminopyridine (DMAP) was used in stoichiometric amount in this reaction. The tri-Boc protected compound upon treatment with potassium carbonate in methanol under reflux selectively deprotected one Boc group on the aniline nitrogen to give the precursor (-)-**33**, which was used for radiosynthesis of (-)-[¹¹C]**24b**.

The radiosynthesis of (-)-[¹¹C]24b was successfully accomplished in two steps from the precursor as shown in Scheme 7. The precursor was first reacted with [¹¹C]CH₃I to obtain the intermediate [¹¹C]methylated Boc protected compound. This intermediate was then treated with trifluoroacetic acid *in situ* to obtain the Boc deprotected product (-)-[¹¹C]24b in high radiochemical yield (40-50%). The new PET radiotracer obtained was subjected to biodistribution evaluations in Sprague–Dawley rats and microPET imaging studies in nonhuman primates.

In Vitro Binding Studies

VAcHT binding was assayed using highly expressed human VAcHT with gently homogenized and partially clarified PC12^{123,7} cells by displacement of bound 5 nM (-)-[³H]vesamicol. Apparent equilibrium dissociation constants (K_i , nM) are reported in Table 1. The K_{i1} and K_{i2} binding affinities were assayed in rat brain and in guinea pig membranes, respectively. Apparent equilibrium dissociation constants (K_i , nM) are reported in Table 1. The ligand selectivity is defined in terms of an index that is the K_i for α_1 or α_2 receptors divided by K_i for VAcHT (K_{i1}/K_{iVAcHT} or K_{i2}/K_{iVAcHT}). A larger number represents good selectivity for binding to VAcHT.

In the previous studies, we had reported that a new class of carbonyl group containing analogues displayed high potency and high selectivity for VAcHT;⁴ particularly, compound (1-(3-hydroxy-1,2,3,4-tetrahydronaphthalen-2-yl)piperidin-4-yl)(thiophen-2-yl)methanone (**9**), which replaces the phenyl group in the structure of compound **5** with a 2-thiophene moiety, displays comparable affinity for VAcHT, with a K_i value of 5.00 ± 1.20 nM. In the current study, to explore the structure-activity relationship, we first replaced the thiophen-2-yl group in compound **9** with 1-methyl-1H-pyrrol-2-yl or 1-methyl-1H-pyrrol-3-yl group to obtain compounds **19a** and **19b**. Both of these two compounds displayed moderately potent binding toward VAcHT with the K_i values of 18.4 ± 2.5 and 26.6 ± 3.8 nM for compounds **19a** and **19b**, respectively (Table 1) for binding to VAcHT. Compared to **9**, compounds **19a** and **19b** displayed about 4-5-fold decrease in affinity for VAcHT. However, the selectivity of **19a** and **19b** for VAcHT versus α_1 receptor reached at least 71-fold and 114-fold respectively. More importantly, these modified structures (with a methyl group on the N-atom of the pyrrole) provide a site for labeling with carbon-11 via [¹¹C]methyl iodide.

When the benzoyl group was replaced with pyridin-3-carbonyl, 6-methyl-pyridin-3-carbonyl, 6-methoxy-pyridin-3-carbonyl, or 6-fluoro-pyridin-3-carbonyl, compounds **19c**, **19d**, **19e**, and **19j** were obtained. The pyridine-3-carbonyl analogue **19c** ($K_i = 24.1 \pm 2.8$ nM) displayed 5-fold lower affinity for VAcHT compared to its benzoyl counterpart **5** ($K_i = 4.30 \pm 1.00$ nM). When the hydrogen on the 6-position of the pyridine-3-carbonyl group is replaced with a methyl group, methoxy group, or fluoride group, the order of the binding potency for VAcHT is $-\text{OCH}_3 > -\text{F} \approx -\text{CH}_3$, with K_i values of 8.36 ± 0.68 , 26.1 ± 2.4 , and 27.9 ± 8.0 nM for compounds **19e**, **19j**, and **19d**, respectively. This demonstrates that an electron donating group, $-\text{OCH}_3$, at the 6-position of pyridin-3-carbonyl results in increased affinity for VAcHT. When further replacing the methoxy in **19e** (K_i value of 8.36 ± 0.68 nM) with fluoroethoxy to afford compound **26a** (K_i value of 38.0 ± 3.8 nM), the affinity for VAcHT decreased 4.5-fold.

When the substitution pattern in the pyridine ring of **19e** is changed from the 6-methoxy-pyridin-3-carbonyl to that of 3-methoxy-pyridin-2-carbonyl (**19f**), binding affinity (K_i value) for VAcHT dropped 15-fold from 8.36 ± 0.68 nM to 121 ± 29 nM. Replacing the methoxy group in **19f** with a fluoroethoxy group to obtain compound **26b** resulted in slight improvement in VAcHT binding (K_i value of 76.4 ± 8.3 nM). The affinities of compounds **19f** and **26b** are lower than those of the structural isomers **19e** and **26a**.

The only difference among compounds **19g**, **19j** and **19k** was the position of fluoro substitution in the pyridin-3-carbonyl group. The order of binding affinity toward VACHT is **19g** \approx **19k** $>$ **19j**, in which the fluorine atom is at 5-, 2- and 6- positions of the pyridine-3-carbonyl ring and the dissociation constants for VACHT are 10.1 ± 1.5 , 12.7 ± 1.1 and 26.1 ± 2.4 nM, respectively. Compounds **19h** and **19i** are *N*-methyl-2-pyridone derivatives. The only difference between them is the position of the bridging carbonyl group located at the 4-position in **19h** and at the 6-position in **19i**. The binding affinities for VACHT are 66.2 ± 10.2 nM for **19h** and 182 ± 65 nM for **19i**.

Compound (4-aminophenyl)(1-(3-hydroxy-1,2,3,4-tetrahydronaphthalen-2-yl)piperidin-4-yl)methanone (**6**) has higher potency for VACHT ($K_i = 1.68 \pm 0.14$ nM) and has suitable lipophilicity (ALog D = 1.56) for crossing the BBB. Introducing methyl group(s) on the aniline nitrogen by *N*-methylation is a conventional way to convert compound **6** into carbon-11 radiolabeled tracer using [^{11}C]methyl iodide. Monomethylation and dimethylation afforded **24a** ($K_i = 0.93 \pm 0.09$ nM) and **24b** ($K_i = 3.03 \pm 0.48$ nM). Their VACHT binding affinities are comparable to that of compound **6** ($K_i = 1.68 \pm 0.14$ nM). The ALog D values of **24a** and **24b** are 3.24 and 2.61 respectively, which suggests they have suitable lipophilicity for the BBB penetration. We experimentally measured the Log D value of **24b** and found to be 2.60.

To test whether an amino group in the 5'-position or 8'-position of the 3'-hydroxy-1',2',3',4'-tetrahydronaphthalen-2'-yl group affects affinity for VACHT, compounds **30a-d** and **31a** were synthesized and their binding affinities were determined. Compound **30a** ($K_i = 38.7 \pm 7.0$ nM) displayed 60-fold higher VACHT binding affinity than that of **31a** ($K_i = 2310 \pm 390$ nM). This result is consistent with the reported results in which the 8'-amino analogues displayed much higher potency than that of 5'-amino analogues.⁴ When aniline compounds **30a**, **30b**, **30c** and **30d** are compared with the non-aniline counterparts, **19a**, **19c**, **19d** and **19e**, there is no any significant change in binding affinities towards VACHT. This suggests that introducing the 5'-amino group into heteroaromatic carbonyl containing analogues may not be beneficial to VACHT binding affinity. Nevertheless, a large difference in binding affinity between the regioisomeric pairs **30a** and **31a** was observed.⁴

These substituted heteroaromatic carbonyl containing VACHT analogues have moderate to high VACHT binding affinities. Consequently, we screened their sigma receptor binding affinity. The *in vitro* data suggest that these new analogues had very low affinities for the sigma receptors. Except for compound **24a** with $K_i = 40.9 \pm 8.2$ nM, all other new analogues exhibit greater than 300 nM for σ_1 receptor, as shown in Table 1. Among these new analogues, 6 compounds **19a**, **19e**, **19g**, **19k**, **24a** and **24b** have K_i values less than 20 nM toward VACHT. Compounds **19a** and **19g** have >70 -fold selectivity ratios for VACHT vs either sigma receptor type. Importantly, compounds **19e**, **19k** and **24b** not only display high affinity toward VACHT with K_i values of 8.36 ± 0.68 , 12.7 ± 1.1 and 3.03 ± 0.48 nM respectively, but they also display greater than 100-fold selectivity ratios for VACHT versus sigma receptors. Compound **24a** has the highest potency for VACHT (0.93 ± 0.09 nM) and is highly selective for VACHT versus σ_1 (44-fold) and σ_2 (4400-fold) receptors. Thus, compound **24a** can be a good blocking agent for validating the selective binding of other VACHT radioligands.

To further test the feasibility of the lead compounds reported in this manuscript to serve as PET tracer for imaging VACHT *in vivo* in living animal, racemic compound **24b** was resolved by HPLC using chiralcel OD column to obtain the (+)-**24b** and (-)-**24b**. The *in vitro* data revealed that (-)-**24b** ($K_i\text{-VACHT} = 0.78$ nM) is the more potent isomer than the (+)-**24b** ($K_i\text{-VACHT} = 19.0$ nM). This is consistent to that ligand binding to VACHT is stereoselective.

In Vivo Evaluation in Rats

To check the *in vivo* distribution of (-)-[¹¹C]24b and its washout kinetics from brain regions of interest and peripheral tissues, ex-vivo biodistribution was conducted in male Sprague-Dawley rats (185 – 205 gram). Rats were euthanized at 5 and 30 min post i.v. injection of (-)-[¹¹C]24b. To test the ability of (-)-[¹¹C]24b to cross the blood brain barrier (BBB), rats were pretreated with Cyclosporine A (CycA) 30 min prior to injection of the radiotracer dose and then euthanized at 30 min post injection of the radiotracer. The distribution data obtained in this study were shown in Figure 3 and 4. For the normal rats, the uptake of radioactivity at 5 min was 0.34, 0.49, 1.77, 0.22, 0.18, 0.89, 1.19, 1.47, 3.45, 0.57 % injected dose per gram (%I.D./g) in blood, heart, lung, muscle, fat, pancreas, spleen, kidney, liver and brain respectively post intravenous (i.v.) injection and the liver has the highest uptake; the radioactivity decreased in all the tissues that were collected in the studies from 5 to 30 min as shown and the liver retained the highest uptake as 2.44 at 30 min. For the rats pretreated with CycA, except the uptake (%I.D./g) in kidney displayed slightly increase (0.77 in control rats, 1.21 in rats pretreated with CycA), the other peripheral tissues didn't show significant change (Figure 3). For the brain regions of interest, the uptake (%I.D./g) at 30 min in cerebellum, striatum, brain stem, cortex, thalamus, hippocampus, and brain were 0.157, 0.593, 0.245, 0.262, 0.293, 0.265 and 0.272 respectively for the control rats; for the rats pretreated with CycA, the uptakes (%I.D.) were 0.404, 1.020, 0.577, 0.637, 0.600, 0.562 and 0.596 respectively for corresponding brain regions of interest. The uptake in brain was observed to increase 2.2-fold when the rats were pretreated with CycA. P-glycoprotein (P-gp) is a 170-kDa protein that is able to binding with compounds with diversify structures and it has widespread tissue distribution belonging to the adenosine triphosphate (ATP)-binding cassette (ABC) transporters^{42, 43} and it is expressed in the capillary endothelial cells which comprise the blood-brain barrier.⁴² CycA, is a modulator/inhibitor of the adenosine triphosphate (ATP)-binding cassette (ABC) transporters including P-gp. It was frequently used to evaluate the ABC transporter-mediated efflux of PET radiotracers and it suggested that ABC transporter-mediated efflux of PET radiotracers has species difference.⁴⁴ If a radioligand is a substrate of P-gp, rats pretreated with CycA will results in significantly increase of the uptake in the brain of animals, for example, radioligands, [¹¹C]verapamil,^{45, 46} [¹¹C]GR218231⁴⁷ and benzamide D₃ radioligands.⁴⁸ For radioligand, (-)-[¹¹C]24b, using CycA pretreated the rats displayed only 2.2-fold increase in the brain uptake of the rats. Considering the brain uptake (%I.D./g) of radioactivity reached 0.57 at 5 min. we concluded that the P-gp modulating the brain uptake of (-)-[¹¹C]24b is very weak and (-)-[¹¹C]24b is able to penetrate the BBB and displayed sufficient uptake in the brain of the rats.

MicroPET Studies in Monkeys

To further confirm that (-)-[¹¹C]24b is able to bind with VAcHT in the brain *in vivo*, microPET studies of (-)-[¹¹C]24b in the brain of nonhuman primate, male cynomolgus monkey were performed (n = 3). The microPET studies demonstrated that (-)-[¹¹C]24b is able to enter the brain and has highest accumulation in striatum, the VAcHT enriched area in the regions of interest in the brain (Figure 5). (-)-[¹¹C]24b is able to give sufficient contrast for the striatum versus other non-target regions. The tissue-time activity curves post injection of (-)-[¹¹C]24b revealed that the radioactivity accumulation was the highest at 10 min post-injection. The ratio of radioactivity accumulation in the target (striatum) and non-target (cerebellum) reaches > 2.5 fold after 70 min post injection (Figure 5). This data suggests that (-)-[¹¹C]24b is a promising PET tracer to quantify VAcHT *in vivo*.

Conclusion

In the present study, we successfully synthesized a series of new VAcHT inhibitors by replacing the benzoyl group in **5** with a heteroaromatic carbonyl group or replacing the 4-aminobenzoyl group with the 4-methylaminobenzoyl group or the 4-*N,N*-dimethylaminobenzoyl group. The six compounds **19a**, **19e**, **19g**, **19k**, **24a** and **24b** displayed high VAcHT binding affinities (K_i values ranging from 0.93 nM to 18.4 nM) and good selectivity for VAcHT over sigma receptors. In particular, compounds **19e**, **19k** and **24b** are very potent for VAcHT with K_i values of 8.36 ± 0.68 , 12.7 ± 1.1 and 3.03 ± 0.48 nM, respectively; and binding selectivity ratios equal to or greater than 100-fold for VAcHT over sigma receptors. The racemate **24b** was successfully resolved on HPLC to obtain the minus and plus isomers. *In vivo* validation of (-)-[^{11}C]**24b** in rodents and nonhuman primates demonstrated that (-)-[^{11}C]**24b** is able to penetrate the BBB and has highest accumulation in the striatum, the VAcHT enriched area in the brain. The time tissue-activity of (-)-[^{11}C]**24b** in the brain of cynomolgus monkey revealed that it has favorable washout pharmacokinetics in the brain. Further imaging studies of (-)-[^{11}C]**24b** in nonhuman primate are warranted to test the feasibility of (-)-[^{11}C]**24b** to be a promising candidate for assessing the level of VAcHT in the brain.

Experimental Section

General

All reagents and chemicals were purchased from commercial suppliers and used without further purification unless otherwise stated. All anhydrous reactions were carried out in oven-dried glassware under an inert nitrogen atmosphere unless otherwise stated. When the reactions involved extraction with methylene chloride (CH_2Cl_2), chloroform (CHCl_3), or ethyl acetate (EtOAc), the organic solutions were dried with anhydrous Na_2SO_4 and concentrated on a rotary evaporator under reduced pressure. Melting points were determined on the MEL-TEMP 3.0 apparatus and left uncorrected. ^1H NMR spectra of majority of the compounds were recorded at 300 MHz on a Varian Mercury-VX spectrometer with CDCl_3 as solvents and tetramethylsilane (TMS) was used as the internal standard. Varian 400 MHz NMR was used for some compounds and was reported in the experimental section where appropriate. Elemental analyses (C, H, N) were determined by Atlantic Microlab, Inc. and were found to be within 0.4% of theoretical values. Chiralcel OD column was used for normal phase HPLC to resolve enantiomers. Phenomenex Luna C18 column was used for reverse phase HPLC conditions to purify the radioactive product on HPLC, and Phenomenex Prodigy was used for QC analysis of radiotracer.

Resolution of (4-aminophenyl)(1-(3-hydroxy-1,2,3,4-tetrahydronaphthalen-2-yl)-piperidin-4-yl)methanone (**6**) to obtain the minus isomer (-)-**6** and the plus isomer (+)-**6**

Approximately 105.0 mg of racemate **6** was resolved on HPLC using a Chiralcel OD column (250 mm \times 10 mm) under isocratic conditions (34% isopropanol in hexane) at a flow rate of 4.0 mL/min and UV wave length at 254 nm to give 41.0 mg of (+)-**6** ($R_t = 20.8$ min) and 48.0 mg of (-)-**6** ($R_t = 33$ min). The specific rotation was determined on an automatic polarimeter (Autopol 111, Rudolph Research, Flanders, NJ). The optical rotation was $[\alpha]_D = -50^\circ$ for (-)-**6** and $[\alpha]_D = +63^\circ$ for (+)-**6** at the concentration of 1.0 mg/mL in dichloromethane at 20 $^\circ\text{C}$.

tert-Butyl 4-(methoxy(methyl)carbamoyl)piperidine-1-carboxylate (**11**)

To a solution of **10** (2.5 g, 10.9 mmol) in CH_2Cl_2 (30 mL) at room temperature, CDI (1.77 g, 11.0 mmol) was added. The mixture was stirred at room temperature for 1 h and *N,N*,*O*-dimethylhydroxylamine hydrochloride (1.3 g, 13.3 mmol) followed by Et_3N were added. The

reaction mixture was stirred overnight and was washed with aqueous Na₂CO₃, water, dried and concentrated under reduced pressure. The residue was purified by silica gel column chromatography to give **11** as a white solid (2.70 g, 90%). mp: 54 °C. ¹H NMR (CDCl₃): 1.46 (s, 9H), 1.64-1.72 (m, 4H), 2.78 (s br, 3H), 3.18 (s, 3H), 3.71 (s, 3H), 4.13 (s br, 2H).

Procedure A: General Method for the Synthesis of Compounds 15h-i

4-Bromo-1-methylpyridin-2(1H)-one (15h)—A solution of 4-bromopyridin-2-amine **12h** (0.60 g, 3.5 mmol) in a mixture of 2 N H₂SO₄ (20 mL) and 2 N NaNO₂ (10 mL) was stirred at 0-5 °C for 2 h. The reaction mixture was extracted with CH₂Cl₂. Crude product was used in the next step without further purification. To the above crude product, potassium carbonate (0.50 g, 3.6 mmol) and methyl iodide (0.53 g, 3.7 mmol) were added and heated at 80 °C in acetone (100 mL) in a sealed tube for 4 h. The reaction mixture was cooled, and potassium carbonate was filtered off. Acetone was evaporated and a small amount of water was added to the residue. This solution was extracted with CH₂Cl₂ and the product was purified with silica gel column chromatography to afford **15h** as a yellow solid (355 mg, 57%). ¹H NMR (CDCl₃): 3.49 (s, 3H), 6.31 (d, *J* = 6.0 Hz, 1H), 6.82 (s, 1H), 7.14 (d, *J* = 6.0 Hz, 1H).

6-Bromo-1-methylpyridin-2(1H)-one (15i)—Compound **15i** as a yellow solid was synthesized starting with compound **12i** as described in procedure A. mp: 105 °C. Yield, 54 %. ¹H NMR (CDCl₃): 3.73 (s, 3H), 6.46-6.52 (m, 2H), 7.10-7.16 (m, 1H).

tert-Butyl 4-(1-methyl-1H-pyrrole-2-carbonyl)piperidine-1-carboxylate (16a)—To a schlenk flask containing *N*-methylpyrrole (0.49 g, 6.08 mmol), 20 mL of THF was added while stirring at room temperature until a clear solution was formed. The solution was cooled down to -78 °C for 15 min and 12.0 mL (6.08 mmol) of *n*-BuLi was added. The solution was allowed to warm up to 0 °C for 20 min, resulting in the formation of the yellow lithium intermediate. The resulting mixture was added via cannula into a solution of **11** (0.83 g, 3.04 mmol) in THF (20 mL) at the same temperature and the reaction mixture was stirred at -78 °C for 4 h, then quenched with saturated aqueous NH₄Cl and allowed to warm to room temperature. The mixture was washed with brine and dried over Na₂SO₄, filtered, and evaporated under reduced pressure to give the crude product. The crude compound was purified by silica gel chromatography to obtain the desired compound **16a** (0.61 g, 34%). ¹H NMR (CDCl₃): 1.47 (s, 9H), 1.66-1.80 (m, 4H), 2.83 (s, 2H), 3.17 (m, 1H), 3.94 (s, 3H), 4.18 (s br, 2H), 6.15 (dd, *J* = 4.2, 2.4 Hz, 1H), 6.84 (pseudo t, *J* = 1.8 Hz, 1H), 6.99 (dd, *J* = 4.2, 1.5 Hz, 1H).

tert-Butyl 4-(1-methyl-1H-pyrrole-4-carbonyl)piperidine-1-carboxylate (16b)—To a solution of 3-bromo-1-methyl-1H-pyrrole (2.19 g, 13.8 mmol) in anhydrous THF at -78 °C, *n*-BuLi (1.6 M, 10 mL) was added. The solution was stirred for 45 minutes at -78 °C. The resulting mixture was cannulated into a solution of **11** (2.5 g, 9.2 mmol) in THF (80 mL) at the same temperature and the reaction mixture was stirred at -78 °C for 4 h, then quenched with sat. aqueous NH₄Cl and allowed to warm to room temperature. The mixture was washed with brine and dried over Na₂SO₄, filtered, and evaporated under reduced pressure to give the crude product. The crude compound was purified by silica gel chromatography to obtain the desired compound **16b** (1.07 g, 40%). ¹H NMR (CDCl₃): 1.47 (s, 9H), 1.66-1.77 (m, 4H), 2.83 (s, 2H), 3.15-3.18 (m, 1H), 3.70 (s, 3H), 4.13 (s br, 2H), 6.57-6.61 (m, 2H), 7.26-7.29 (m, 1H).

tert-Butyl 4-nicotinoylpiperidine-1-carboxylate (16c)—To a solution of 3-bromopyridine (1.13 g, 7.2 mmol) in anhydrous THF (45 mL) at -40 °C under argon atmosphere, lithium dibutyl(isopropyl)magnesate (5.2 mL, 0.7 M, 3.6 mmol) was added.

Stirring was continued at the same temperature for 1 h. The resulting mixture was cannulated into a solution of **11** (1.5 g, 5.5 mmol) in THF (50 mL) at -78 °C. The solution was maintained at -78 °C for 1 h, and quenched with saturated aqueous NH₄Cl and allowed to warm to room temperature. The organic layer was separated, and the aqueous layer was extracted with ethyl acetate. The combined organic layers were washed with water, dried over Na₂SO₄, filtered, and evaporated under reduced pressure to give the crude product. The crude compound was purified by silica gel chromatography to obtain the desired compound **16c** (0.49 g, 31%). ¹H NMR (CDCl₃): 1.47 (s, 9H), 1.63-1.89 (m, 4H), 2.92 (m, 2H), 3.38 (m, 1H), 4.20 (m, 2H), 7.44 (ddd, *J* = 8.1, 5.1, 0.9 Hz, 1H), 8.22 (dt, *J* = 8.1, 2.1 Hz, 1H), 8.79 (dd, *J* = 5.1, 1.8 Hz, 1H), 9.16 (d, *J* = 1.8 Hz, 1H).

tert-Butyl 4-(6-methylnicotinoyl)piperidine-1-carboxylate (16d)—Compound **16d** was prepared from 5-bromo-2-methylpyridine following the procedure described above for the preparation of **16c**. Yield, 42%. ¹H NMR (CDCl₃): 1.49 (s, 9H), 1.68-1.87 (m, 4H), 2.63 (s, 3H), 2.90 (m, 2H), 3.35 (m, 1H), 4.18 (s br, 2H), 7.28 (d, *J* = 8.4 Hz, 1H), 8.11 (dd, *J* = 8.4, 2.1 Hz, 1H), 9.04 (d, *J* = 2.1 Hz, 1H).

tert-Butyl 4-(6-methoxynicotinoyl)piperidine-1-carboxylate (16e)—Compound **16e** was prepared from 5-bromo-2-methoxypyridine following the procedure described above for the preparation of **16b**. Yield, 61%. ¹H NMR (CDCl₃): 1.47 (s, 9H), 1.62-1.86 (m, 4H), 2.88 (m, 2H), 3.31 (m, 1H), 4.01 (s, 3H), 4.19 (s br, 2H), 6.81 (d, *J* = 8.7 Hz, 1H), 8.13 (dd, *J* = 8.7, 2.4 Hz, 1H), 8.79 (d, *J* = 2.4 Hz, 1H).

tert-Butyl 4-(3-methoxypicolinoyl)piperidine-1-carboxylate (16f)—Compound **16f** was prepared from 2-bromo-3-methoxypyridine following the procedure described above for the preparation of **16b**. Yield, 36%. ¹H NMR (CDCl₃): 1.47 (s, 9H), 1.66-1.87 (m, 4H), 2.89 (s, 2H), 3.67-3.81 (m, 1H), 3.90 (s, 3H), 4.07 (s br, 2H), 7.35-7.45 (m, 2H), 8.23-8.25 (m, 1H).

tert-Butyl 4-(3-fluoronicotinoyl)piperidine-1-carboxylate (16g)—Compound **16g** was prepared from 3-bromo-5-fluoropyridine following the procedure described above for the preparation of **16b**. Yield, 41%. ¹H NMR (CDCl₃): 1.44 (s, 9H), 1.56-1.61 (m, 2H), 1.86-1.90 (m, 2H), 2.87 (s, 2H), 3.17-3.24 (m, 1H), 4.06 (s br, 2H), 7.54-7.58 (m, 1H), 8.53-8.60 (m, 2H).

tert-Butyl 4-(1-methyl-2-oxo-1,2-dihydropyridine-4-carbonyl)piperidine-1-carboxylate (16h)—Compound **16h** was prepared from compound **15h** following the procedure described above for the preparation of **16b**. Yield, 38%. ¹H NMR (CDCl₃): 1.47 (s, 9H), 1.56-1.87 (m, 4H), 2.82 (s, 2H), 3.05-3.07 (m, 1H), 3.50 (s, 3H), 4.17 (s br, 2H), 6.49 (d, *J* = 6.0 Hz, 1H), 6.73 (d, *J* = 6.0 Hz, 1H), 7.36 (s, 1H).

tert-Butyl 4-(1-methyl-6-oxo-1,6-dihydropyridine-2-carbonyl)piperidine-1-carboxylate (16i)—Compound **16i** was prepared from compound **15i** following the procedure described above for the preparation of **16b**. Yield, 35%. ¹H NMR (CDCl₃): 1.45 (s, 9H), 1.58-1.87 (m, 4H), 2.81 (s, 2H), 3.05-3.07 (m, 1H), 3.47 (s, 3H), 4.14 (s br, 2H), 6.44-6.47 (m, 1H), 6.69-6.72 (m, 1H), 7.30-7.36 (m, 1H).

Procedure B: General Method for Synthesis of Compounds 17a-i

(1-Methyl-1H-pyrrol-2-yl)(piperidin-4-yl)methanone (17a)—To a solution of **16a** (0.67 g, 2.3 mmol) in CH₂Cl₂ (30 mL), TFA (2 mL) was added. The reaction mixture was stirred at room temperature for 4 h. The solvent was removed under reduced pressure and the residue was neutralized with 1 N NaOH solution and extracted with CH₂Cl₂ (2 × 15

mL). The organic layer was washed with brine, dried and concentrated to give crude product. The crude product was purified by silica gel column chromatography to afford **17a** (0.32 g, 72%). ¹H NMR (CDCl₃): 1.76-1.87 (m, 4H), 2.81 (m, 2H), 3.17-3.23 (m, 4H), 3.94 (s, 3H), 6.14 (m, 1H), 6.83 (m, 1H), 6.98 (m, 1H).

(1-Methyl-1H-pyrrol-3-yl)(piperidin-4-yl)methanone (17b)—Compound **17b** was prepared from compound **16b** as described in procedure B. Yield, 80%. ¹H NMR (CDCl₃): 1.76-1.80 (m, 4H), 2.65-2.73 (m, 2H), 3.01-3.17 (m, 4H), 3.68 (s, 3H), 6.57-6.59 (m, 2H), 7.25 (s, 1H).

Piperidin-4-yl(pyridin-3-yl)methanone (17c)—Compound **17c** was prepared from compound **16c** as described in procedure B. Yield, 85%. ¹H NMR (CDCl₃): 1.62-1.77 (m, 2H), 1.86-1.89 (m, 3H), 2.79 (td, *J* = 12.6, 2.7 Hz, 2H), 3.21 (dt, *J* = 12.9, 3.0 Hz, 2H), 3.37 (tt, *J* = 11.4, 3.9 Hz, 1H), 7.43 (ddd, *J* = 8.1, 4.8, 0.9 Hz, 1H), 8.22 (ddd, *J* = 4.8, 2.1, 1.5 Hz, 1H), 8.78 (dd, *J* = 4.5, 1.5 Hz, 1H), 9.16 (dd, *J* = 2.4, 0.9 Hz, 1H).

(6-Methylpyridin-3-yl)(piperidin-4-yl) methanone (17d)—Compound **17d** was prepared from compound **16d** as described in procedure B. Yield, 70%. ¹H NMR (CDCl₃): 1.62-1.87 (m, 5H), 2.63 (s, 3H), 2.77 (m, 2H), 3.16-3.22 (m, 2H), 3.33 (m, 1H), 7.27 (d, *J* = 8.4 Hz, 1H), 8.12 (dd, *J* = 8.1, 2.4 Hz, 1H), 9.04 (d, *J* = 2.4 Hz, 1H).

(6-Methoxypyridin-3-yl)(piperidin-4-yl)methanone (17e)—Compound **17e** was prepared from compound **16e** as described in procedure B. Yield, 77%. ¹H NMR (CDCl₃): 1.65-1.89 (m, 4H), 2.40 (s, 1H), 2.78 (td, *J* = 12.0, 2.7 Hz, 2H), 3.21 (dt, *J* = 9.0, 3.6 Hz, 2H), 3.31 (m, 1H), 4.00 (s, 3H), 6.79 (d, *J* = 8.4 Hz, 1H), 8.13 (dd, *J* = 8.4, 2.4 Hz, 1H), 8.78 (d, *J* = 2.4 Hz, 1H).

(3-Methoxypyridin-2-yl)(piperidin-4-yl)methanone (17f)—Compound **17f** was prepared from compound **16f** as described in procedure B. Yield, 78%. ¹H NMR (CDCl₃): 1.51-1.81 (m, 4H), 2.69 (s, 2H), 3.08-3.25 (m, 3H), 3.49-3.58 (m, 1H), 3.83 (s, 3H), 7.27-7.36 (m, 2H), 8.16-8.18 (m, 1H).

(5-Fluoropyridin-3-yl)(piperidin-4-yl)methanone (17g)—Compound **17g** was prepared from compound **16g** as described in procedure B. Yield, 79%. ¹H NMR (CDCl₃): 1.56-1.61 (m, 2H), 1.86-1.90 (m, 2H), 2.87 (m, 2H), 3.17-3.21 (m, 4H), 7.56 (s, 1H), 8.53-8.60 (m, 2H).

1-Methyl-5-(piperidine-4-carbonyl)pyridin-2(1H)-one (17h)—Compound **17h** was prepared from compound **16h** as described in procedure B. Yield, 79%. ¹H NMR (CDCl₃): 1.57-1.88 (m, 4H), 2.83 (s, 2H), 3.03-3.09 (m, 4H), 3.50 (s, 3H), 6.50 (d, *J* = 6.0 Hz, 1H), 6.72 (d, *J* = 6.0 Hz, 1H), 7.38 (s, 1H).

1-Methyl-6-(piperidine-4-carbonyl)pyridin-2(1H)-one (17i)—Compound **17i** was prepared from compound **16i** as described in procedure B. Yield, 75%. ¹H NMR (CDCl₃): 1.58-1.87 (m, 4H), 2.82 (s, 2H), 3.02-3.10 (m, 4H), 3.47 (s, 3H), 6.42-6.48 (m, 1H), 6.67-6.72 (m, 1H), 7.31-7.36 (m, 1H).

Procedure C: General Method of Preparing (19a-i) and Their Corresponding Oxalates

(1-(3-Hydroxy-1,2,3,4-tetrahydronaphthalen-2-yl)piperidin-4-yl)(1-methyl-1H-pyrrol-2-yl)methanone (19a)—A mixture of **17a** (0.27 g, 1.4 mmol), **18** (0.10 g, 0.68 mmol) and Et₃N (0.3 mL, 2.2 mmol) in ethanol (5 mL) was stirred at 75 °C for 36 h. After cooling to room temperature, the reaction mixture was poured into water and extracted with

EtOAc (3 × 15 mL). The residue was purified by silica gel column chromatography to give **19a** as a white solid (0.11 g, 47%). ¹H NMR (CDCl₃, free base): 1.81-2.03 (m, 4H), 2.37 (m, 1H), 2.76-3.13 (m, 8H), 3.30 (m, 1H), 3.88 (m, 1H), 3.95 (s, 3H), 4.45 (s br, 1H), 6.14 (m, 1H), 6.83 (m, 1H), 6.98 (m, 1H), 7.09-7.16 (m, 4H). Free base was converted to the corresponding oxalate salt by adding oxalic acid in ethyl acetate to **19a** in CH₂Cl₂. mp: 212 °C (decomposed). Anal. (C₂₁H₂₆N₂O₂ • H₂C₂O₄) C, H, N.

(1-(3-Hydroxy-1,2,3,4-tetrahydronaphthalen-2-yl)piperidin-4-yl)(1-methyl-1H-pyrrol-3-yl)methanone (19b)—Compound **19b** was prepared from compound **17b** as described in procedure C. Yield, 50%. ¹H NMR (CDCl₃, free base): 1.83-2.00 (m, 4H), 2.38 (m, 1H), 2.76-3.13 (m, 8H), 3.29-3.35 (m, 1H), 3.71 (s, 3H), 4.32 (s br, 1H), 6.61 (m, 2H), 7.12-7.16 (m, 4H), 7.30-7.31 (m, 1H). The free base was converted to the oxalate salt. mp: 212.6 °C (decomposed). Anal. (C₂₁H₂₆N₂O₂ • H₂C₂O₄•0.25H₂O) C, H, N.

(1-(3-Hydroxy-1,2,3,4-tetrahydronaphthalen-2-yl)piperidin-4-yl)(pyridin-3-yl)methanone (19c)—Compound **19c** was prepared from compound **17c** as described in procedure C. Yield, 40%. ¹H NMR (CDCl₃, free base): 1.77-1.98 (m, 4H), 2.43 (m, 1H), 2.75-3.02 (m, 7H), 3.20-3.38 (m, 2H), 3.88 (m, 1H), 7.08-7.15 (m, 4H), 7.42-7.46 (m, 1H), 8.21-8.25 (m, 1H), 8.77-8.79 (m, 1H), 9.16 (s, 1H). The free base was converted to the oxalate salt. mp: 214 °C (decomposed). Anal. (C₂₁H₂₄N₂O₂ • H₂C₂O₄) C, H, N.

(1-(3-Hydroxy-1,2,3,4-tetrahydronaphthalen-2-yl)piperidin-4-yl)(6-methoxypyridin-3-yl)methanone (19d)—Compound **19d** was prepared from compound **17d** as described in procedure C. Yield, 44%. ¹H NMR (CDCl₃, free base): 1.80-2.02 (m, 4H), 2.43 (m, 1H), 2.62 (s, 3H), 2.78-3.06 (m, 7H), 3.20-3.38 (m, 2H), 3.89 (m, 1H), 6.83 (d, *J* = 8.7 Hz, 1H), 7.11-7.18 (m, 4H), 8.17 (dd, *J* = 8.7, 2.4 Hz, 1H), 8.82 (d, *J* = 2.4 Hz, 1H). The free base was converted to the oxalate salt. mp: 223 °C (decomposed). Anal. (C₂₂H₂₆N₂O₂ • 2H₂C₂O₄) C, H, N.

(1-(3-Hydroxy-1,2,3,4-tetrahydronaphthalen-2-yl)piperidin-4-yl)(6-methylpyridin-3-yl)methanone (19e)—Compound **19e** was prepared from compound **17e** as described in procedure C. Yield, 42%. ¹H NMR (CDCl₃, free base): 1.74-1.96 (m, 4H), 2.41 (m, 1H), 2.75-3.01 (m, 7H), 3.26-3.33 (m, 2H), 3.86 (m, 1H), 4.04 (s, 3H), 4.17 (s br, 1H), 7.06-7.14 (m, 4H), 7.27 (d, *J* = 8.1 Hz, 1H), 8.11 (dd, *J* = 8.1, 2.1 Hz, 1H), 9.03 (d, *J* = 2.1 Hz, 1H). The free base was converted to the oxalate salt. mp: 240 °C (decomposed). Anal. (C₂₂H₂₆N₂O₃ • H₂C₂O₄) C, H, N.

(1-(3-Hydroxy-1,2,3,4-tetrahydronaphthalen-2-yl)piperidin-4-yl)(3-methoxypyridin-2-yl)methanone (19f)—Compound **19f** was prepared from compound **17f** as described in procedure C. Yield, 36%. ¹H NMR (CDCl₃, free base): 1.72-1.96 (m, 4H), 2.33-2.41 (m, 1H), 2.72-2.96 (m, 7H), 3.26-3.33 (m, 1H), 3.55-3.63 (m, 1H), 3.81-3.90 (m, 3H), 4.30 (s br, 1H), 7.06-7.14 (m, 4H), 7.26-7.39 (m, 2H), 8.23-8.25 (m, 1H). The free base was converted to the oxalate salt. mp: 146.6 °C (decomposed). Anal. (C₂₂H₂₆N₂O₃ • H₂C₂O₄•0.25H₂O) C, H, N.

(5-Fluoropyridin-3-yl)(1-(3-hydroxy-1,2,3,4-tetrahydronaphthalen-2-yl)piperidin-4-yl)methanone (19g)—Compound **19g** was prepared from compound **17g** as described in procedure C. Yield, 44%. ¹H NMR (CDCl₃, free base): 1.70-2.04 (m, 4H), 2.34-2.43 (m, 1H), 2.75-3.34 (m, 8H), 3.82-3.90 (m, 1H), 4.13 (s br, 1H), 7.06-7.11 (m, 4H), 7.57-7.61 (m, 1H), 8.56-8.62 (m, 2H). The free base was converted to the oxalate salt. mp: 203.7 °C (decomposed). Anal. (C₂₁H₂₃FN₂O₂ • H₂C₂O₄) C, H, N.

4-(1-(3-Hydroxy-1,2,3,4-tetrahydronaphthalen-2-yl)piperidine-4-carbonyl)-1-methylpyridin-2(1H)-one (19h)—Compound **19h** was prepared from compound **17h** as described in procedure C. Yield, 37%. ¹H NMR (CDCl₃, free base): 1.72-1.99 (m, 4H), 2.33-2.39 (m, 1H), 2.75-3.01 (m, 6H), 3.27-3.34 (m, 2H), 3.50 (s, 3H), 3.82-3.91 (m, 1H), 4.08 (s br, 1H), 6.45 (d, *J* = 6.0 Hz, 1H), 6.72 (d, *J* = 6.0 Hz, 1H), 7.12-7.13 (m, 4H), 7.35 (s, 1H). The free base was converted to the oxalate salt. mp: 93.8 °C (decomposed). Anal. (C₂₂H₂₆N₂O₃•H₂C₂O₄•1.5H₂O) C, H, N.

6-(1-(3-Hydroxy-1,2,3,4-tetrahydronaphthalen-2-yl)piperidine-4-carbonyl)-1-methylpyridin-2(1H)-one (19i)—Compound **19i** was prepared from compound **17i** as described in procedure C. Yield, 39%. ¹H NMR (CDCl₃, free base): 1.72-2.04 (m, 4H), 2.32-2.39 (m, 1H), 2.81-3.01 (m, 6H), 3.27-3.35 (m, 2H), 3.50 (s, 3H), 3.82-3.89 (m, 1H), 4.06 (s br, 1H), 6.43-6.46 (m, 1H), 6.70-6.73 (m, 1H), 7.06-7.14 (m, 4H), 7.31-7.37 (m, 1H). The free base was converted to the oxalate salt. mp: 122.4 °C (decomposed). Anal. (C₂₂H₂₆N₂O₃•H₂C₂O₄•1.5H₂O) C, H, N.

Procedure D: General Method for the Synthesis of Compounds (19j-k) and Their Corresponding Oxalates

(6-Fluoropyridin-3-yl)(1-(3-hydroxy-1,2,3,4-tetrahydronaphthalen-2-yl)piperidin-4-yl)methanone (19j)—To a solution of **17j** (2.42 g, 13.8 mmol) in anhydrous THF at -78 °C, *n*-BuLi (1.6 M, 10 mL) was added. The solution was stirred for 45 minutes at -78 °C. The resulting mixture was cannulated into a solution of **21** (3.97 g, 9.2 mmol) in THF (80 mL) at the same temperature and the reaction mixture was stirred at -78 °C for 4 h, then quenched with sat. aqueous NH₄Cl and allowed to warm to room temperature. The mixture was washed with brine and dried over Na₂SO₄, filtered, and evaporated under reduced pressure to give the crude product. The crude compound was purified by chromatography on silica gel to obtain the TBDMS-protected intermediate (1-(3-(*tert*-butyldimethylsilyloxy)-1,2,3,4-tetrahydronaphthalen-2-yl)piperidin-4-yl)(6-fluoropyridin-3-yl) methanone (1.55 g, 36%). ¹H NMR (CDCl₃): 0.12 (s, 6H), 0.91 (s, 9H), 1.65-1.77 (m, 4H), 2.46-3.05 (m, 9H), 4.13 (s br, 2H), 7.04-7.12 (m, 4H), 8.23-8.37 (m, 2H), 8.78 (s, 1H).

A mixture of the intermediate (1-(3-(*tert*-butyldimethylsilyloxy)-1,2,3,4-tetrahydronaphthalen-2-yl)piperidin-4-yl)(6-fluoropyridin-3-yl) methanone (1.55 g, 3.3 mmol) and concentrated HCl (5 mL) in THF were stirred for 4 h at room temperature until TLC indicated that deprotection was complete, and then it was carefully neutralized with 1 N NaOH and extracted with CH₂Cl₂. The crude product was purified by column chromatography to afford **19j** as white solid (0.92 g, 79%). ¹H NMR (CDCl₃, free base): 1.84-2.03 (m, 4H), 2.38-2.46 (m, 1H), 2.75-3.02 (m, 6H), 3.21-3.34 (m, 2H), 3.82-3.89 (m, 1H), 4.30 (s br, 1H), 7.03-7.11 (m, 4H), 8.33-8.39 (m, 2H), 8.79 (s, 1H). Free base was converted to the corresponding oxalate salt by adding oxalic acid in ethyl acetate to **19j** in CH₂Cl₂. mp: 204.3 °C (decomposed). Anal. (C₂₁H₂₃FN₂O₂•H₂C₂O₄•0.5H₂O) C, H, N.

(2-Fluoropyridin-3-yl)(1-(3-hydroxy-1,2,3,4-tetrahydronaphthalen-2-yl)piperidin-4-yl)methanone (19k)—Compound **19k** was prepared from compound **17k** as describe in procedure D to give TBDMS-protected intermediate (1-(3-(*tert*-butyldimethylsilyloxy)-1,2,3,4-tetrahydronaphthalen-2-yl)piperidin-4-yl)(2-fluoropyridin-3-yl) methanone (1.68 g, 39%). ¹H NMR (CDCl₃): 0.11 (s, 6H), 0.90 (s, 9H), 1.63-1.78 (m, 4H), 2.45-3.08 (m, 9H), 4.13 (s br, 2H), 7.04-7.11 (m, 4H), 7.31-7.39 (m, 1H), 8.23-8.30 (m, 1H), 8.38-8.40 (m, 1H). Removal of TBDMS with HCl gave **19k** (0.87 g, 75%). ¹H NMR (CDCl₃, free base): 1.84-2.03 (m, 4H), 2.38-2.46 (m, 1H), 2.75-2.99 (m, 6H), 3.25-3.33 (m, 2H), 3.80-3.90 (m, 1H), 4.31 (s br, 1H), 7.03-7.13 (m, 4H), 7.30-7.41 (m,

1H), 8.22-8.31 (m, 1H), 8.38-8.40 (m, 1H). The free base was converted to the oxalate salt. mp: 205.8 °C (decomposed). Anal. (C₂₁H₂₃FN₂O₂•H₂C₂O₄•H₂O) C, H, N.

1-(3-Hydroxy-1,2,3,4-tetrahydronaphthalen-2-yl)-N-methoxy-N-methylpiperidine-4-carboxamide (20)—TFA (2 mL) was added into a solution of **11** (0.38 g, 1.4 mmol) in CH₂Cl₂ (30 mL). The reaction mixture was stirred at room temperature for 4 h. The solvent was removed under reduced pressure and the residue was neutralized with 1 N NaOH solution and extracted with CH₂Cl₂ (2 × 15 mL). The organic layer was washed with brine, dried and concentrated to give the crude compound, which was used in the next step without further purification. Crude compound, **18** (0.10 g, 0.68 mmol) and Et₃N (0.3 mL, 2.2 mmol) in ethanol (5 mL) were stirred at 75 °C for 36 h. After cooling to room temperature, the reaction mixture was poured into water and extracted with EtOAc (3 × 15 mL). The organic layer was dried and concentrated under reduced pressure. The residue was purified by silica gel column chromatography to give **20** as a white solid (86.4 mg, 40%). ¹H NMR (CDCl₃): 1.81-1.93 (m, 4H), 2.28-2.31 (m, 1H), 2.75-2.97 (m, 8H), 3.27-3.20 (s, 3H), 3.27-3.34 (m, 1H), 3.72 (s, 3H), 3.85-3.90 (m, 1H), 4.27 (s br, 1H), 7.09-7.13 (m, 4H).

1-(3-((tert-Butyldimethylsilyloxy)-1,2,3,4-tetrahydronaphthalen-2-yl)-N-methoxy-N-methylpiperidine-4-carboxamide (21)—To a solution of **20** (0.4 g, 1.25 mmol) and imidazole (0.4 g, 5.88 mmol) in CH₂Cl₂ (50 mL), TBDMSCl (0.38 g, 2.5 mmol) was added. The reaction mixture was stirred overnight at room temperature until TLC indicated that the reaction was complete. The reaction mixture was washed with brine and 1 N NaH₂PO₄ (30 mL × 3). The organic layer was dried and concentrated to a residue. The crude product was purified by silica gel column chromatography to afford **21** as a white solid (0.38 g, 70 %). ¹H NMR (CDCl₃): 0.12 (s, 6H), 0.91 (s, 9H), 1.65-1.77 (m, 4H), 2.46-3.05 (m, 9H), 3.17 (s, 3H), 3.69 (s, 3H), 4.13 (s br, 2H), 7.04-7.12 (m, 4H).

3-(4-(4-Acetamidobenzoyl)piperidin-1-yl)-1,2,3,4-tetrahydronaphthalen-2-yl acetate (22)—Acetic anhydride (1.89 mL, 18.5 mmol) was added dropwise over 15 min to a magnetically stirred solution of **6** (0.54 g, 1.54 mmol) and Et₃N (3.12 g, 30.8 mmol) in dry CH₂Cl₂ (10 mL) overnight. The reaction was monitored by TLC. After the reaction was complete, the solvent was evaporated under reduced pressure. Water was added to wash the resulting solid and the residue was purified by silica gel column chromatography (ethyl acetate: hexane = 3:2) to give **22** (0.55 g, 82%). ¹H NMR (CDCl₃): 1.24-1.28 (m, 2H), 1.70-1.84 (m, 2H), 2.12 (s, 3H), 2.22 (s, 3H), 2.44-2.60 (m, 2H), 2.84-3.05 (m, 6H), 3.16-3.23 (m, 2H), 5.27-5.34 (m, 1H), 7.05-7.16 (m, 4H), 7.49 (s br, 1H), 7.62 (d, *J* = 8.4 Hz, 2H), 7.92 (d, *J* = 8.4 Hz, 2H).

N-(4-(1-(3-Hydroxy-1,2,3,4-tetrahydronaphthalen-2-yl)piperidine-4-carbonyl)phenyl)-N-methylacetamide (23)—Sodium hydride (96 mg, 2.4 mmol) was added to 3-(4-(4-acetamidobenzoyl)piperidin-1-yl)-1,2,3,4-tetrahydronaphthalen-2-yl acetate **22** (0.87 g, 2 mmol) in anhydrous THF, and iodomethane (0.34 g, 2.4 mmol) was added dropwise to the mixture, which was maintained below 5 °C for 0.5 h and then stirred at room temperature for 1 h. The reaction was monitored by TLC. After the reaction was complete, the mixture was partitioned between saturated aqueous NH₄Cl and ethyl acetate. The organic layer was separated and the aqueous layer was extracted with ethyl acetate. The combined organic layers dried and concentrated. The crude product was purified by silica gel column chromatography (ethyl acetate: hexane = 3:2) to give **23** (0.63 g, 78%). ¹H NMR (CDCl₃): 1.77-1.90 (m, 4H), 1.96 (s, 3H), 2.44 (t, *J* = 10.3 Hz, 1H), 2.76-3.03 (m, 7H),

3.27-3.35 (m, 2H), 3.31 (s, 3H), 3.84-3.89 (m, 1H), 4.21 (s br, 1H), 7.09-7.28 (m, 4H), 7.32 (d, $J = 8.1$ Hz, 2H), 8.01 (d, $J = 7.8$ Hz, 2H).

(4-(Dimethylamino)phenyl)(1-(3-hydroxy-1,2,3,4-tetrahydronaphthalen-2-yl)piperidin-4-yl)methanone (24a)—Sodium hydride (96 mg, 2.4 mmol) was added to **6** (0.87 g, 2 mmol) in anhydrous THF, and iodomethane (4.8 mmol) was added dropwise to the mixture, which was stirred at room temperature for 0.5 h. The reaction was monitored by TLC. After the reaction was complete, the mixture was partitioned between saturated aqueous NH_4Cl and ethyl acetate. The organic layer was separated and the aqueous layer was extracted with ethyl acetate. The combined organic layers were dried and concentrated. The crude product was purified by silica gel column chromatography to give **24a** as a white solid (0.63 g, 83%). $^1\text{H NMR}$ (CDCl_3 , free base): 1.81-1.98 (m, 4H), 2.36-2.44 (m, 1H), 2.74-3.06 (m, 13H), 3.23-3.33 (m, 2H), 3.83-3.91 (m, 1H), 4.46 (s br, 1H), 6.66 (d, $J = 9$ Hz, 2H), 7.09-7.15 (m, 4H), 7.88 (d, $J = 9$ Hz, 2H). Free base was converted to the corresponding oxalate salt by adding oxalic acid in ethyl acetate to **24a** in CH_2Cl_2 . mp: 228.9 °C (decomposed). Anal. ($\text{C}_{24}\text{H}_{30}\text{N}_2\text{O}_2 \cdot \text{H}_2\text{C}_2\text{O}_4$) C, H, N.

(1-(3-Hydroxy-1,2,3,4-tetrahydronaphthalen-2-yl)piperidin-4-yl)(4-(methylamino)phenyl) methanone (24b)—Concentrated HCl (12 M, 0.25 mL) was added to a stirred solution of **23** (0.4 g, 1.0 mmol) in ethylene glycol (0.75 mL). The reaction mixture was heated to reflux for 3 h and the reaction was monitored by TLC. When the reaction was complete, the mixture was partitioned between water and ethyl acetate. The organic layer was separated and the aqueous layer was extracted. The combined organic layers dried and concentrated. The crude product was purified by silica gel column chromatography (ethyl acetate/hexane, 1/4) to give **24b** (0.3 g, 82%). $^1\text{H NMR}$ (CDCl_3): 1.85-1.92 (m, 4H), 2.40-2.44 (m, 1H), 2.77-2.99 (m, 8H), 3.27-3.34 (m, 2H), 3.81-3.89 (m, 2H), 4.19-4.23 (m, 1H), 4.46 (s br, 1H), 6.59 (d, $J = 8.1$ Hz, 2H), 7.09-7.15 (m, 4H), 7.86 (d, $J = 8.1$ Hz, 2H). Free base was converted to the corresponding oxalate salt by adding oxalic acid in ethyl acetate to **24b** in CH_2Cl_2 . mp: 215.7 °C (decomposed). Anal. ($\text{C}_{23}\text{H}_{28}\text{N}_2\text{O}_2 \cdot \text{H}_2\text{C}_2\text{O}_4$) C, H, N.

Resolution of (1-(3-Hydroxy-1,2,3,4-tetrahydronaphthalen-2-yl)piperidin-4-yl)(4-(methylamino)phenyl) methanone (24b) to obtain the enantiomerically minus isomer, (-)-24b and plus isomer (+)-24b—Approximately 200 mg of (\pm)-**24b** was separated on chiral HPLC using a Chiralcel OD column (250 mm \times 10mm). The mobile phase used was 35% isopropanol in hexane at a flow rate of 4.0 mL/min to give 83.3 mg of (+)-**24b** ($R_t = 15$ min) and 94.9 mg of (-)-**24b** ($R_t = 30$ min). The specific rotation was determined on an automatic polarimeter (Autopol 111, Rudolph Research, Flanders, NJ). The optical rotation of (-)-**24b** was $[\alpha]_D = -30.5^\circ$ at the concentration of 1.8 mg/mL in dichloromethane and that of (+)-**24b** was $[\alpha]_D = +21.8^\circ$ at the concentration of 1.1 mg/mL in dichloromethane at 20 °C. The (-)-**24b** and (+)-**24b** were converted to oxalates by treating one equivalent of (-)-**24b** or (+)-**24b** with one equivalent of oxalic acid. The salt obtained was used for the *in vitro* studies. mp of (+)-**24b**: 199.8 °C (decomposed), mp of (-)-**24b**: 200.2 °C (decomposed).

(1--3-Hydroxy-1,2,3,4-tetrahydronaphthalen-2-yl)piperidin-4-yl)(6-hydroxypyridin-3-yl)methanone (25)—Into an oven-dried argon-purged 50 mL round bottom flask was placed **19e** (73.3 mg, 0.2 mmol) and 3.0 mL chloroform was added followed by TMSI (57 μL , 0.4 mmol). The reaction mixture was heated to 55 °C for 1 h until TLC (EtOAc/hexane, 1/1) indicated the disappearance of starting material. The reaction mixture was cooled to room temperature and 0.6 mL methanol was added. The reaction mixture was concentrated. Ethyl acetate was added followed by aqueous sodium

bicarbonate solution. The ethyl acetate layer was separated and the aqueous layer was extracted with ethyl acetate. Combined organic layers were washed with brine, dried over anhydrous sodium sulfate, and concentrated to give compound **25** as a white solid (69 mg, 97%). ¹H NMR (CDCl₃): 1.40-2.00 (m, 3H), 2.20-2.25 (m, 1H), 2.60-3.10 (m, 8H), 3.30 (dd, *J* = 6.2, 13.9 Hz, 1H), 3.80-4.00 (m, 1H), 4.20-4.25 (m, 1H), 6.60 (d, *J* = 9.6 Hz, 1H), 7.00-7.20 (m, 4 H), 8.05 (dd, *J* = 2.7, 9.6 Hz, 1H), 8.16 (s, 1H).

(6-(2-Fluoroethoxy)pyridin-3-yl)(1-(3-hydroxy-1,2,3,4-tetrahydronaphthalen-2-yl)-piperidin-4-yl)methanone (26a)—To the mixture of **25** (69 mg, 0.195 mmol) and 1-bromo-2-fluoroethane (30 μL, 0.4 mmol) in DMF (2 mL) was added potassium carbonate (60 mg, 0.43 mmol). The resultant reaction mixture was stirred at the room temperature for 72 h. Ethyl acetate was added to the reaction mixture and washed with aqueous sodium bicarbonate solution. The organic layer was dried over anhydrous sodium sulfate and concentrated. The crude product was purified by silica gel chromatography to give colorless sticky solid (40 mg, 51%). ¹H NMR (CDCl₃): 1.75 -1.99 (m, 1H), 2.20 - 2.50 (m, 1H), 2.70-3.10 (m, 11H), 3.30 (dd, *J* = 16.0, 6.0 Hz, 1H), 3.80-3.95 (m, 1H), 4.27 (t, *J* = 4.5 Hz, 1H), 4.36 (t, *J* = 4.5 Hz, 1H), 4.67 (t, *J* = 4.5 Hz, 1H), 4.83 (t, *J* = 4.5 Hz, 1H), 6.61 (d, *J* = 9.6 Hz, 1H), 7.00-7.20 (m, 4H), 7.88 (dd, *J* = 2.7, 9.6 Hz, 1H), 8.15 (s, 1H). Free base was converted to the corresponding oxalate salt by adding oxalic acid in ethyl acetate to **26a** in CH₂Cl₂. mp: 84 °C (decomposed). Anal. (C₂₄H₂₇FN₂O₃•H₂C₂O₄•H₂O) C, H, N.

(3-(2-Fluoroethoxy)pyridin-2-yl)(1-(3-hydroxy-1,2,3,4-tetrahydronaphthalen-2-yl)piperidin-4-yl)methanone (26b)—To a solution of **28** (1.60 g, 7.3 mmol) in THF was added *n*-BuLi (1.6 M, 7 mL) at -78 °C under N₂ atmosphere. The solution was stirred at -78 °C for 1 h and a solution of *tert*-butyl-4-(methoxy(methyl)carbamoyl)piperidine-1-carboxylate **11** (1.0 g, 3.6 mmol) in THF was added. The solution was maintained at -78 °C for 4 h, and then quenched with saturated aqueous NH₄Cl that was allowed to warm to room temperature with stirring. The organic layer was separated and the aqueous layer was extracted with ethyl acetate. The combined extracts were washed with water, dried over Na₂SO₄, filtered, concentrated, and the residue chromatographed on a silica gel column with ethyl acetate : hexane (1:4, v/v) to give the *t*-Boc protected compound *tert*-butyl-4-(3-(2-fluoroethoxy)picolinoyl)piperidine-1-carboxylate (0.51 g, 40%), ¹H NMR (CDCl₃): 1.47 (s, 9H), 1.62-1.70 (m, 4H), 2.83 (s, 2H), 3.64-3.73 (m, 1H), 4.17 (s br, 2H), 4.25-4.36 (m, 2H), 4.68-4.87 (m, 2H), 7.23-7.26 (m, 1H), 7.38-7.40 (m, 1H), 8.25-8.30 (m, 1H).

To a solution of the above compound (0.49 g, 1.4 mmol) in CH₂Cl₂ (30 mL), TFA (2 mL) was added. The reaction mixture was stirred at room temperature for 4 h. The solvent was removed under reduced pressure, and the residue was neutralized with 1 N NaOH solution and extracted with CH₂Cl₂ (2 × 15 mL). The organic layer was washed with brine, dried and concentrated to give crude 4-(3-(2-fluoroethoxy)picolinoyl)piperidine. The crude product was used in the next step without further purification.

A mixture of the above compound, **18** (0.10 g, 0.68 mmol) and Et₃N (0.3 mL, 2.2 mmol) in ethanol (5 mL) was stirred at 75 °C for 36 h. After cooling to room temperature, the mixture was poured into water, extracted with EtOAc (3 × 15 mL). The organic layer was dried and concentrated under reduced pressure. The residue was purified by silica gel column chromatography to give **26b** (0.12 g, 43%). ¹H NMR (CDCl₃, free base): 1.73-1.98 (m, 4H), 2.32-2.40 (m, 1H), 2.71-2.96 (m, 8H), 3.31-3.33 (m, 1H), 3.49-3.56 (m, 1H), 3.80-3.89 (m, 1H), 4.24-4.36 (m, 2H), 4.69-4.87 (m, 2H), 7.09-7.25 (m, 4H), 7.34-7.38 (m, 2H), 8.27-8.29 (m, 1H). The corresponding oxalate salt was obtained by adding oxalic acid in ethyl acetate the solution of **26b** in CH₂Cl₂ and then recrystallized. For the oxalate salt, mp: 119.9 °C (decomposed). Anal. (C₂₃H₂₇FN₂O₃•H₂C₂O₄•H₂O) C, H, N.

2-Bromo-3-(2-fluoroethoxy)pyridine (28)—A mixture of 2-bromopyridin-3-ol **27** (0.17 g, 1.0 mmol), 1-bromo-2-fluoroethane (0.25 g, 2.0 mmol) and K_2CO_3 (0.55 g, 4.0 mmol) in acetonitrile were stirred at reflux for one day until TLC indicated that the reaction was complete. The reaction mixture was filtered, dried and concentrated under reduced pressure. The crude product was purified by silica gel column chromatography to afford **28** (0.16 g, 68%). 1H NMR ($CDCl_3$): 4.25-4.34 (m, 2H), 4.73-4.89 (m, 2H), 7.20-7.22 (m, 2H), 8.01 (s, 1H).

Procedure E: General Method of Preparing 30a, 30c-d and 31a

(1-(8-Amino-3-hydroxy-1,2,3,4-tetrahydronaphthalen-2-yl)piperidin-4-yl)(1-methyl-1Hpyrrol-2-yl)methanone (30a)—A mixture of **29** (0.20 g, 0.78 mmol), **17a** (0.44 g, 2.3 mmol) and Et_3N (0.5 mL) in ethanol (10 mL) was stirred at 60 °C for 48 h. To the mixture, 1 N NaOH (3 mL) was added and the stirring was continued overnight. The solvent was removed, the residue was extracted with EtOAc (3 × 30 mL) and the organic layer was washed with aqueous Na_2CO_3 solution, dried and concentrated. The crude product was purified by column chromatography to give **30a** (0.11 g, 37%). 1H NMR ($CDCl_3$, free base): 1.85-1.96 (m, 4H), 2.43-2.53 (m, 2H), 2.67-2.89 (m, 5H), 2.96-3.28 (m, 3H), 3.60 (s br, 2H), 3.85 (m, 1H), 3.95 (s, 3H), 6.14 (m, 1H), 6.57 (m, 2H), 6.83 (s br, 1H), 6.96-7.02 (m, 2H). Free base was converted to the corresponding oxalate salt by adding oxalic acid in ethyl acetate to **30a** in CH_2Cl_2 . mp: 131 °C (decomposed). Anal. ($C_{21}H_{27}N_3O_2 \cdot 2H_2C_2O_4 \cdot 2H_2O$) C, H, N.

(1-(8-Amino-3-hydroxy-1,2,3,4-tetrahydronaphthalen-2-yl)piperidin-4-yl)(pyridin-3-yl)methanone (30c)—Compound **30c** was prepared from compound **17c** as described in procedure E. Yield, 61%. 1H NMR ($CDCl_3$, free base): 1.80-2.05 (m, 4H), 2.36-2.53 (m, 2H), 2.68-2.92 (m, 5H), 3.01-3.35 (m, 4H), 3.61 (s br, 2H), 3.87 (m, 1H), 6.54-6.60 (m, 2H), 6.99 (td, $J = 7.5, 3.3$ Hz, 1H), 7.45 (dd, $J = 8.1, 4.8$ Hz, 1H), 8.24 (dt, $J = 8.1, 1.8$ Hz, 1H), 8.80 (dd, $J = 4.8, 1.8$ Hz, 1H), 9.17 (d, $J = 2.1$ Hz, 1H). The free base was converted to the oxalate salt. mp: 109 °C (decomposed). Anal. ($C_{21}H_{25}N_3O_2 \cdot 2H_2C_2O_4 \cdot 0.5H_2O$) C, H, N.

(1-(8-Amino-3-hydroxy-1,2,3,4-tetrahydronaphthalen-2-yl)piperidin-4-yl)(6-methylpyridin-3-yl)methanone (30d)—Compound **30d** was prepared from compound **17d** as described in procedure E. Yield, 44%. 1H NMR ($CDCl_3$, free base): 1.79-1.99 (m, 5H), 2.35-2.53 (m, 2H), 2.64 (s, 3H), 2.67-3.28 (m, 8H), 3.62 (s br, 2H), 3.87 (m, 1H), 6.57 (m, 2H), 6.99 (m, 1H), 7.29 (d, $J = 8.1$ Hz, 1H), 8.13 (dd, $J = 8.1, 2.1$ Hz, 1H), 9.04 (d, $J = 2.1$ Hz, 1H). The free base was converted to the oxalate salt. mp: 98 °C (decomposed). Anal. ($C_{24}H_{29}N_3O_4 \cdot H_2C_2O_4$) C, H, N.

(1-(8-Amino-3-hydroxy-1,2,3,4-tetrahydronaphthalen-2-yl)piperidin-4-yl)(6-methoxypyridin-3-yl)methanone (30e)—Compound **30e** was prepared from compound **17e** as describe in procedure E. Yield, 43%. 1H NMR ($CDCl_3$, free base): 1.65 (s br, 1H), 1.80-2.02 (m, 4H), 2.42-2.53 (m, 2H), 2.67-3.03 (m, 6H), 3.21-3.28 (m, 2H), 3.61 (s br, 2H), 3.86 (m, 1H), 4.02 (s, 3H), 6.57 (m, 2H), 6.82 (d, $J = 8.7$ Hz, 1H), 6.99 (t, $J = 7.8$ Hz, 1H), 8.15 (dd, $J = 8.7, 2.4$ Hz, 1H), 8.80 (d, $J = 2.4$ Hz, 1H). The free base was converted to the oxalate salt. mp: 81.4 °C (decomposed). Anal. ($C_{22}H_{27}N_3O_3 \cdot 2H_2C_2O_4 \cdot 1.5H_2O$) C, H, N.

(1-(5-Amino-3-hydroxy-1,2,3,4-tetrahydronaphthalen-2-yl)piperidin-4-yl)(1-methyl-1H-pyrrol-2-yl)methanone (31a)—Compound **31a** was prepared from compound **17a** as describe in procedure E. Yield, 20%. 1H NMR ($CDCl_3$, free base): 1.85-1.96 (m, 4H), 2.36-2.45 (m, 2H), 2.76-2.89 (m, 5H), 2.96-3.16 (m, 3H), 3.62 (s br, 2H), 3.92 (m, 1H), 3.96 (s, 3H), 6.15 (m, 1H), 6.56 (m, 2H), 6.83 (s br, 1H), 6.96- 7.02 (m, 2H).

The free base was converted to the oxalate salt. mp: 114 °C (decomposed). Anal. (C₂₁H₂₇N₃O₂ • 2H₂C₂O₄ • 1.5H₂O) C, H, N.

tert-Butyl (4-(3-hydroxy-1,2,3,4-tetrahydronaphthalen-2-yl)piperidine-4-carbonyl)phenyl)-carbamate, (-)-33—To a solution of (-)-6 (153.6 mg, 0.438 mmol) in THF was added Di-*tert*-butyl dicarbonate (Boc₂O, 287.0 mg, 1.314 mmol), Et₃N (0.5 mL) and DMAP (5.4 mg, 0.044 mmol). The reaction mixture was stirred at room temperature while monitoring by TLC. After 1.5 hrs the starting material completely disappeared, at which point the reaction mixture was concentrated on Rotary evaporator and partitioned the residue with brine and ethyl acetate. Aqueous phase was washed with ethyl acetate. The organic phase was dried over sodium sulfate, concentrated and purified on silica gel column (8:1 to 6:1 hexanes: ethyl acetate) to give the tri-Boc protected intermediate (-)-32 which was dissolved in methanol and excess K₂CO₃ was added and refluxed overnight. The product was partitioned between brine and dichloromethane. Aqueous phase was washed twice with dichloromethane. The organic phase was dried over sodium sulfate and concentrated to give (-)-33 as a white solid in 28% yield. ¹H NMR (400 MHz, CDCl₃): 1.55 (s, 9H), 1.78-1.95 (m, 4H), 2.42 (t, *J* = 12.0 Hz, 1H), 2.78-3.05 (m, 7H), 3.25-3.35 (m, 2H), 3.83-3.90 (m, 1H), 6.73 (s, 1H), 7.08-7.07 (m, 4H), 7.46 (d, *J* = 11.6 Hz, 2H), 7.92 (d, *J* = 12.4 Hz, 2H).

Radiochemistry

[¹¹C]CH₃I was produced at our institution from [¹¹C]CO₂ using a GE PETtrace MeI Microlab. Up to 1.4 Ci of [¹¹C]CO₂ was produced from Washington University's JSW BC-16/8 cyclotron by irradiating a gas target of 0.5% O₂ in N₂ for 15-30 min with a 40 μA beam of 16 MeV protons. The GE PETtrace MeI microlab converts the [¹¹C]CO₂ to [¹¹C]CH₄ using a nickel catalyst (Shimalite-Ni, Shimadzu, Japan P.N.221-27719) in the presence of hydrogen gas at 360 °C; it was further converted to [¹¹C]CH₃I by reaction with iodine that was held in a column in the gas phase at 690 °C. Several hundred millicuries of [¹¹C]CH₃I were delivered as a gas at approximately 12 min after end of bombardment (EOB), to the hot cell where the radiosynthesis was accomplished.

Radiosynthesis of (-)-[¹¹C]24b—Approximately 1.2 - 1.5 mg of (-) enantiomer of the precursor was placed in a reaction vessel and 0.2 mL of DMF was added followed by 3.0 μL of 5N aqueous sodium hydroxide. The mixture was thoroughly mixed on a vortex. [¹¹C]CH₃I was bubbled into the reaction vessel. The reaction mixture was heated at 85 °C for 5 min. The reaction vessel was removed from heating, and 200 μL trifluoroacetic acid was added. The reaction vessel was mixed well and heated again at 85 °C for 5 min, and then quenched by adding 1.4 mL of HPLC mobile phase (29% acetonitrile in 0.1M ammonium formate buffer pH 4.5) and 200 μL 5N aqueous NaOH to neutralize the reaction mixture. The solution was loaded on to reverse phase C-18 column (Phenomenex Luna C18, 250mm × 9.6 mm, 10 μm with UV wave length at 254 nm); using the above HPLC mobile phase, at a flow rate of 4.0 ml/min, the radioactive product was collected between 17.0 and 19.0 min, and diluted with 50 mL of sterile water. The aqueous solution was passed through C18 Sep-Pak Plus (to trap the product) by applying nitrogen pressure. The collection bottle was rinsed by adding 10 mL water and passed through Sep-Pak plus. The product was collected in a vial by eluting C18 Sep-Pak plus with 0.6 mL of EtOH and 5.4 mL of saline to formulate the injection dose. The injection dose sample was authenticated using analytical HPLC system by co-injecting with cold standard compound (-)-24b. The HPLC system for quality control is: Column: Phenomenex Prodigy C18 analytical column, 250 × 4.6 mm; Mobile phase: 37% acetonitrile in 0.1 M ammonium formate buffer pH=4.5; Flow rate: 1.2 mL/min; the retention time for (-)-[¹¹C]-24b was 4.9 min. The entire process was completed in approximately 1 hr. The radiochemical yield was 40-50% (decay corrected).

to EOB) with the radiochemical purity of > 99% and the specific activity was > 2000 Ci/mmol (decay corrected to end of synthesis).

Log D Measurement

Partition coefficient was measured by mixing the (-)-[¹¹C]24b sample with 3 mL each of 1-octanol and buffer that is 0.1 M phosphate and pH equals 7.4 in a test tube. The mixture in the test tube were vortexed for 20 s followed by centrifugation for 1 min at room temperature. 2 mL of organic layer was transferred to a second test tube, 1 mL 1-octanol and 3 mL PBS buffer was added. The resulting mixture was vortexed for 20 s followed by centrifugation for 1 min at room temperature. 1 mL of organic and aqueous layer were taken separately for measurement. The radioactivity content values (count per minute) of two samples (1 mL each) from the 1-octanol and buffer layers were counted in a gamma-counter. The partition coefficient Log D_{7.4} was determined by calculating as the decimal logarithm the ratio of cpm/mL of 1-octanol to that of buffer. The measurements were repeated three times. Value of partition coefficient is 2.60.

In Vitro Biological Evaluation

Vesicular acetylcholine transporter binding assays—*In vitro* binding assays to VACHT were conducted with human VACHT permanently expressed in PC12 cells at about 50 pmol/mg of crude extract. No significant amounts of α_1 or α_2 receptors were present. The radioligand used was 5 nM (-)-[³H]vesamicol, and the assay was conducted at final concentrations of 10⁻¹¹ M to 10⁻⁵ M novel compounds.^{4, 19} Unlabeled (-)-vesamicol was used as an external standard, for which K_i = 15 nM, and the mixture was allowed to equilibrate at 23 °C for 20 hours. Duplicate data were averaged and fitted by regression of a rectangular hyperbola to estimate the K_i value of the novel compounds.

Sigma receptor binding assays—The compounds were dissolved in DMF, DMSO or ethanol, and diluted in 50 mM Tris-HCl buffer containing 150 mM NaCl and 100 mM EDTA at pH 7.4 prior to performing the α_1 and α_2 receptor binding assays. The detailed procedures for performing the binding assays have been described.^{19, 49} For the α_1 receptor assays, guinea pig brain membrane homogenates (~300 µg protein) were the receptor resource and ~5 nM (+)-[³H] pentazocine (34.9 Ci/mmol, Perkin-Elmer, Boston, MA) was the radioligand. The incubation was performed in 96-well plates for 90 min at room temperature. Nonspecific binding was determined from samples that contained 10 µM of nonradioactive haloperidol. After 90 min, the reaction was quenched by addition of 150 µL of ice-cold wash buffer (10 mM Tris-HCl, 150 mM NaCl, pH 7.4). The harvested samples were filtered rapidly through a 96-well fiberglass filter plate (Millipore, Billerica, MA) that had been presoaked with 100 µL of 50 mM Tris-HCl buffer at pH 8.0 for 60 min. Each filter was washed 3 × 200 µL of ice-cold wash buffer, and the filter counted in a Wallac 1450 MicroBeta liquid scintillation counter (Perkin-Elmer, Boston, MA). The α_2 receptor binding assays were determined using rat liver membrane homogenates (~300 µg protein) and ~5 nM [³H]DTG (58.1 Ci/mmol, Perkin-Elmer, Boston, MA) in the presence of 1 µM of (+)-pentazocine to block α_1 sites. The incubation time was 120 min at room temperature. Nonspecific binding was determined from samples that contained 10 µM of nonradioactive haloperidol. All other procedures were same as those described for the α_1 receptor binding assay above.

The IC₅₀ value was determined using nonlinear regression analysis. Competitive curves were best fit with a one-site model and gave pseudo-Hill coefficients of 0.6-1.0. K_i values were calculated using the method of Cheng and Prusoff⁵⁰ and are presented as the mean (± 1 SEM). For these calculations, we used a K_D value of 7.89 nM for [³H](+)-pentazocine

binding to α_1 receptor in guinea pig brain and a K_d value of 30.7 nM for [^3H]DTG binding to α_2 receptor in rat liver.

Biodistribution in Rats

All animal experiments were conducted in compliance with the Guidelines for the Care and Use of Research Animals established by Washington University's Animal Studies Committee. For the biodistribution studies, ~350 μCi of (-)-[^{11}C]24b in about 175 μL of 10% ethanol/saline solution (v/v) was injected *via* the tail vein into mature male Sprague–Dawley rats (185 - 205 g) under anesthesia (2.5% isoflurane in oxygen at a flow rate of 1 mL/min). A group of at least four rats were used for each time point. For the control group, at 5 and 30 min post injection, the rats were anesthetized and euthanized. For the CycA pretreated group, CycA (Sandimmune diluted 1:1 with saline) at a dose of 25 mg/kg were administered by intravenously (i.v.) 30 min prior to radioligand injection; at 30 min post injection of the radioligand, (-)-[^{11}C]24b, the rats were euthanized. The whole brain was quickly harvested and various organs dissected comprising cerebellum, brain stem, cortex, striatum, thalamus, hippocampus and the brain. The remainder of the brain was also collected in order to determine total brain uptake. Simultaneously, samples of blood, heart, lung, liver, spleen, pancreas, kidney, muscle, fat, and tail were dissected. All the tissue samples were collected in the tared tubes and counted in an automated gamma counter (Beckman Gamma 8000 well counter) along with the standard solution of (-)-[^{11}C]24b prepared by diluting the injectate. The counted tissues were then weighed, and the %ID/g was calculated.

MicroPET Studies in Nonhuman Primate Brain

A microPET Focus 220 scanner (Concorde/CTI/Siemens Microsystems, Knoxville, TN) was used for the imaging studies of (-)-[^{11}C]24b in male cynomolgus monkey (4–6 kg). The animals were fasted for 12 h before the study. The animals were initially anesthetized using an intramuscular injection with ketamine (10 mg/kg) and glycopyrulate (0.13 mg/kg), and intubated with an endotracheal tube under anesthesia (maintained at 0.75–2.0% isoflurane in oxygen) throughout the PET scanning procedure. After intubation, a percutaneous venous catheter was placed for radiotracer injection. A 10 min transmission scan was performed to check the positioning; once confirmed, a 45 min transmission scan was obtained for attenuation correction. After that, the animal was administered 5–7 mCi of (-)-[^{11}C]-24b *via* the venous catheter. Subsequently, a 100 min dynamic PET scan (3 \times 1 min, 4 \times 2 min, 3 \times 3 min, and 20 \times 5 min) was acquired. During the whole procedure, core temperature was kept constant at 37 $^\circ\text{C}$ with a heated water blanket. In each microPET scanning session, the head was positioned supine in the adjustable head holder with the brain in the center of the field of view. For each subject, at least three independent PET studies were performed (n = 3).

MicroPET Image Data Processing and Analysis

PET image reconstructed resolution was < 2.0 mm full width half maximum for all 3 dimensions at the center of the field of view. Emission scans were corrected using individual attenuation and model-based scatter correction and reconstructed using filtered back projection as described previously.⁵¹ The first baseline PET image for each animal acted as the target image with the MPRAGE MRI scan and subsequent PETs coregistered to it using automated image registration program AIR.^{52, 53} All MPRAGE-based volume of interest (VOI) analyses were done by investigators blinded to the clinical status of the monkeys.⁴ For quantitative analyses, three-dimensional regions of interest (ROI) (cerebellum, frontal, occipital, striatum, temporal, white matter, midbrain and hippocampus) were transformed to the baseline PET space and then overlaid on all reconstructed PET images to obtain time–

activity curves. Activity measures were standardized to body weight and dose of radioactivity injected to yield standardized uptake value (SUV).

Supplementary Material

Refer to Web version on PubMed Central for supplementary material.

Acknowledgments

Research reported in this publication was supported by the National Institute Of Neurological Disorders And Stroke of the National Institutes of Health under Award Number R01NS075527, NS061025, The National Institute of Mental Health (NIMH) under Award Number MH092797, and McDonnell Center for Systems Neuroscience of Washington University at St. Louis.

References

1. http://www.alz.org/downloads/facts_figures_2012.pdf.
2. Qiu C, De Ronchi D, Fratiglioni L. The epidemiology of the dementias: an update. *Curr Opin Psychiatry*. 2007; 20:380–385. [PubMed: 17551353]
3. Klunk WE, Engler H, Nordberg A, Wang Y, Blomqvist G, Holt DP, Bergstrom M, Savitcheva I, Huang G, Estrada S, Ausen B, Debnath ML, Barletta J, Price JC, Sandell J, Lopresti BJ, Wall A, Koivisto P, Antoni G, Mathis CA, Langstrom B. Imaging brain amyloid in Alzheimer's disease with Pittsburgh Compound-B. *Ann Neurol*. 2004; 55:306–319. [PubMed: 14991808]
4. Efsange SM, Khare AB, von Hohenberg K, Mach RH, Parsons SM, Tu Z. Synthesis and in vitro biological evaluation of carbonyl group-containing inhibitors of vesicular acetylcholine transporter. *J Med Chem*. 2010; 53:2825–2835. [PubMed: 20218624]
5. Masliah E, Mallory M, Hansen L, Alford M, DeTeresa R, Terry R, Baudier J, Saitoh T. Localization of amyloid precursor protein in GAP43-immunoreactive aberrant sprouting neurites in Alzheimer's disease. *Brain Res*. 1992; 574:312–316. [PubMed: 1386275]
6. Davies P, Maloney AJF. Selective loss of central cholinergic neurons in alzheimers-disease. *Lancet*. 1976; 2:1403–1403. [PubMed: 63862]
7. Dekosky ST, Scheff SW. Synapse loss in frontal-cortex biopsies in alzheimers-disease - correlation with cognitive severity. *Ann Neurol*. 1990; 27:457–464. [PubMed: 2360787]
8. Masliah E, Ellisman M, Carragher B, Mallory M, Young S, Hansen L, Deteresa R, Terry RD. 3-Dimensional analysis of the relationship between synaptic pathology and neuropil threads in alzheimer-disease. *J Neuropathol Exp Neurol*. 1992; 51:404–414. [PubMed: 1619440]
9. Peterson DA, Sejnowski TJ, Poizner H. Convergent evidence for abnormal striatal synaptic plasticity in dystonia. *Neurobiol Dis*. 2010; 37:558–573. [PubMed: 20005952]
10. Hilker R, Thomas AV, Klein JC, Weisenbach S, Kalbe E, Burghaus L, Jacobs AH, Herholz K, Heiss WD. Dementia in parkinson disease - functional imaging of cholinergic and dopaminergic pathways. *Neurology*. 2005; 65:1716–1722. [PubMed: 16344512]
11. Castell X, Diebler MF, Tomasi M, Bigaria C, De Gois S, Berrard S, Mallet J, Israel M, Dolezal M. More than one way to toy with ChAT and VAcHT. *J Physiol Paris*. 2002; 96:61–72. [PubMed: 11755784]
12. Breakefield XO, Blood AJ, Li Y, Hallett M, Hanson PI, Standaert DG. The pathophysiological basis of dystonias. *Nat Rev Neurosci*. 2008; 9:222–234. [PubMed: 18285800]
13. Kuhl DE, Fessler JA, Minoshima S, Cho K, Frey KA, Wieland DM, Koeppe RA. In-vivo mapping of cholinergic neurons in the human brain using SPECT and IBVM. *J Nucl Med*. 1994; 35:405–410. [PubMed: 8113884]
14. Bohnen NI, Frey KA. Imaging of cholinergic and monoaminergic neurochemical changes in neurodegenerative disorders. *Mol Imaging Biol*. 2007; 9:243–257. [PubMed: 17318670]
15. Albin RL, Cross D, Cornblath WT, Wald JA, Wernette K, Frey KA, Minoshima S. Diminished striatal [I-123]iodobenzovesamicol binding in idiopathic cervical dystonia. *Ann Neurol*. 2003; 53:528–532. [PubMed: 12666122]

16. Barret O, Mazere J, Seibyl J, Allard M. Comparison of noninvasive quantification methods of in vivo vesicular acetylcholine transporter using [I-123]-IBVM SPECT imaging. *J Cereb Blood Flow Metab.* 2008; 28:1624–1634. [PubMed: 18506194]
17. Rahmim A, Zaidi H. PET versus SPECT: strengths, limitations and challenges. *Nucl Med Commun.* 2008; 29:193–207. [PubMed: 18349789]
18. Jansen FP, Vanderheyden JL. The future of SPECT in a time of PET. *Nucl Med Biol.* 2007; 34:733–735. [PubMed: 17921025]
19. Tu Z, Efange SMN, Xu J, Li S, Jones LA, Parsons SM, Mach RH. Synthesis and in vitro and in vivo evaluation of F-18-labeled positron emission tomography (PET) ligands for imaging the vesicular acetylcholine transporter. *J Med Chem.* 2009; 52:1358–1369. [PubMed: 19203271]
20. Sorger D, Scheunemann M, Vercouillie J, Grossmann U, Fischer S, Hiller A, Wenzel B, Roghani A, Schliebs R, Steinbach J, Brust P, Sabri O. Neuroimaging of the vesicular acetylcholine transporter by a novel 4-[F-18]fluoro-benzoyl derivative of 7-hydroxy-6-(4-phenyl-piperidin-1-yl)-octahydro-benzo[1,4]oxazines. *Nucl Med Biol.* 2009; 36:17–27. [PubMed: 19181265]
21. Kilbourn MR, Hockley B, Lee L, Sherman P, Quesada C, Frey KA, Koeppe RA. Positron emission tomography imaging of (2R,3R)-5-[F-18] fluoroethoxybenzovesamicol in rat and monkey brain: a radioligand for the vesicular acetylcholine transporter. *Nuc Med Biol.* 2009; 36:489–493.
22. Zea-Ponce Y, Mavel S, Assaad T, Kruse SE, Parsons SM, Emond P, Chalon S, Giboureau N, Kassiou M, Guilloteau D. Synthesis and in vitro evaluation of new benzovesamicol analogues as potential imaging probes for the vesicular acetylcholine transporter. *Bioorg Med Chem.* 2005; 13:745–753. [PubMed: 15653342]
23. Scheunemann M, Sorger D, Wenzel B, Heinitz K, Schliebs R, Klingner M, Sabri O, Steinbach J. Synthesis of novel 4- and 5-substituted benzyl ether derivatives of vesamicol and in vitro evaluation of their binding properties to the vesicular acetylcholine transporter site. *Bioorg Med Chem.* 2004; 12:1459–1465. [PubMed: 15018919]
24. Wenzel B, Li Y, Kraus W, Sorger D, Sabri O, Brust P, Steinbach J. Pyrrolovesamicols-synthesis, structure and VACHT binding of two 4-fluorobenzoyl regioisomers. *Bioorg Med Chem Lett.* 2012; 22:2163–2166. [PubMed: 22365760]
25. Sluder A, Shah S, Cassayre J, Clover R, Maienfisch P, Molleyres LP, Hirst EA, Flemming AJ, Shi M, Cutler P, Stanger C, Roberts RS, Hughes DJ, Flury T, Robinson MP, Hillesheim E, Pitterna T, Cederbaum F, Worthington PA, Crossthwaite AJ, Windass JD, Currie RA, Earley FGP. Spiroindolines identify the vesicular acetylcholine transporter as a novel target for insecticide action. *Plos One.* 2012; 7:e34712. [PubMed: 22563457]
26. Kozaka T, Uno I, Kitamura Y, Miwa D, Ogawa K, Shiba K. Syntheses and in vitro evaluation of decalinvesamicol analogues as potential imaging probes for vesicular acetylcholine transporter (VACHT). *Bioorg Med Chem.* 2012; 20:4936–4941. [PubMed: 22831799]
27. Giboureau N, Som IM, Boucher-Arnold A, Guilloteau D, Kassiou M. PET radioligands for the vesicular acetylcholine transporter (VACHT). *Curr Top Med Chem.* 2010; 10:1569–1583. [PubMed: 20583990]
28. Kilbourn MR, Hockley B, Lee L, Koeppe RA. Successful [F-18]FEOBV imaging of the VACHT in monkey brain. *Neuroimage.* 2008; 41:T93–T93.
29. Mach RH, Voytko ML, Ehrenkauf RLE, Nader MA, Tobin JR, Efange SMN, Parsons SM, Gage HD, Smith CR, Morton TE. Imaging of cholinergic terminals using the radiotracer [¹⁸F](+)-4-fluorobenzyltrozamicol: In vitro binding studies and positron emission tomography studies in nonhuman primates. *Synapse.* 1997; 25:368–380. [PubMed: 9097396]
30. Waterhouse RN. Determination of lipophilicity and its use as a predictor of blood-brain barrier penetration of molecular imaging agents. *Mol Imaging Biol.* 2003; 5:376–389. [PubMed: 14667492]
31. Waring MJ. Lipophilicity in drug discovery. *Expert Opin Drug Discov.* 2010; 5:235–248. [PubMed: 22823020]
32. Fichert T, Yazdani M, Proudfoot JR. A structure-permeability study of small drug-like molecules. *Bioorg Med Chem Lett.* 2003; 13:719–722. [PubMed: 12639566]
33. Pajouhesh H, Lenz GR. Medicinal chemical properties of successful central nervous system drugs. *NeuroRx.* 2005; 2:541–553. [PubMed: 16489364]

34. Tu Z, Wang W, Cui J, Zhang X, Lu X, Xu J, Parsons SM. Synthesis and evaluation of in vitro bioactivity for vesicular acetylcholine transporter inhibitors containing two carbonyl groups. *Bioorg Med Chem.* 2012; 20:4422–4429. [PubMed: 22739089]
35. Padakanti PK, Wang R, Kil K, Li S, Perlmutter JS, Zeng D, Mach RH, Parsons SM, Tu Z. Radiosynthesis and in vivo evaluation of (-)-[¹¹C]TZ1-27-2 as a PET tracer for imaging VACHT. *J Nucl Med.* 2011; 52(Supplement 1):223.
36. Pampillon C, Claffey J, Hogan M, Tacke M. Novel achiral titanocene anti-cancer drugs synthesised from bis-*N,N*-dimethylamino fulvene and lithiated heterocyclic compounds. *Biomaterials.* 2008; 21:197–204. [PubMed: 17665139]
37. Forlani L, Cristoni G, Boga C, Todesco PE, Del Vecchio E, Selva S, Monari M. Reinvestigation of the tautomerism of some substituted 2-hydroxypyridines. *Arkivoc.* 2002:198–215.
38. Frank J, Katritzky AR. Tautomeric pyridines .15. pyridone-hydroxypyridine equilibria in solvents of differing polarity. *J Chem Soc Perkin Trans.* 1976; 2:1428–1431.
39. Kuzuya M, Noguchi A, Kamiya S, Okuda T. Reactions of 1-unsubstituted tautomeric 2-pyridones with benzyne. *Chem Pharm Bull.* 1985; 33:2313–2322.
40. Rogers GA, Parsons SM, Anderson DC, Nilsson LM, Bahr BA, Kornreich WD, Kaufman R, Jacobs RS, Kirtman B. Synthesis, in vitro acetylcholine-storage-blocking activities, and biological properties of derivatives and analogs of trans-2-(4-phenylpiperidino) cyclohexanol (vesamicol). *J Med Chem.* 1989; 32:1217–1230. [PubMed: 2724295]
41. Peng Y, Liu H, Tang M, Cai L, Pike V. Highly efficient *N*-monomethylation of primary aryl amines. *Chin J Chem.* 2009; 27:1339–1344.
42. Loscher W, Potschka H. Blood-brain barrier active efflux transporters: ATP-binding cassette gene family. *NeuroRx.* 2005; 2:86–98. [PubMed: 15717060]
43. Pearce HL, Winter MA, Beck WT. Structural characteristics of compounds that modulate P-glycoprotein-associated multidrug resistance. *Adv Enzyme Regul.* 1990; 30:357–373. [PubMed: 1976291]
44. Syvanen S, Lindhe O, Palner M, Kornum BR, Rahman O, Langstrom B, Knudsen GM, Hammarlund-Udenaes M. Species differences in blood-brain barrier transport of three positron emission tomography radioligands with emphasis on P-glycoprotein transport. *Drug Metab Dispos.* 2009; 37:635–643. [PubMed: 19047468]
45. Ishiwata K, Kawamura K, Yanai K, Hendrikse NH. In vivo evaluation of P-glycoprotein modulation of 8 PET radioligands used clinically. *J Nucl Med.* 2007; 48:81–87. [PubMed: 17204702]
46. Luurtsema G, Molthoff CF, Schuit RC, Windhorst AD, Lammertsma AA, Franssen EJ. Evaluation of (R)-[¹¹C]verapamil as PET tracer of P-glycoprotein function in the blood-brain barrier: kinetics and metabolism in the rat. *Nucl Med Biol.* 2005; 32:87–93. [PubMed: 15691665]
47. de Vries EF, Kortekaas R, van Waarde A, Dijkstra D, Elsinga PH, Vaalburg W. Synthesis and evaluation of dopamine D3 receptor antagonist [¹¹C]-GR218231 as PET tracer for P-glycoprotein. *J Nucl Med.* 2005; 46:1384–1392. [PubMed: 16085598]
48. Tu Z, Li S, Xu J, Chu W, Jones LA, Luedtke RR, Mach RH. Effect of cyclosporin A on the uptake of D₃-selective PET radiotracers in rat brain. *Nucl Med Biol.* 2011; 38:725–739. [PubMed: 21718948]
49. Tu Z, Xu J, Jones LA, Li S, Dumstorff C, Vangveravong S, Chen D, Wheeler KT, Welch MJ, Mach RH. Fluorine-18-labeled benzamide analogues for imaging the α_2 receptor status of solid tumors with positron emission tomography. *J Med Chem.* 2007; 50:3194–3204. [PubMed: 17579383]
50. Cheng Y, Prusoff WH. Relationship between inhibition constant (K_i) and concentration of inhibitor which causes 50 per cent inhibition (IC_{50}) of an enzymatic-reaction. *Biochem Pharmacol.* 1973; 22:3099–3108. [PubMed: 4202581]
51. Criswell SR, Perlmutter JS, Videen TO, Moerlein SM, Flores HP, Birke AM, Racette BA. Reduced uptake of [¹⁸F]FDOPA PET in asymptomatic welders with occupational manganese exposure. *Neurology.* 2011; 76:1296–1301. [PubMed: 21471467]

52. Tabbal SD, Mink JW, Antenor JA, Carl JL, Moerlein SM, Perlmutter JS. 1-Methyl-4-phenyl-1,2,3,6-tetrahydropyridine-induced acute transient dystonia in monkeys associated with low striatal dopamine. *Neuroscience*. 2006; 141:1281–1287. [PubMed: 16766129]
53. Woods RP, Mazziotta JC, Cherry SR. MRI-PET registration with automated algorithm. *J Comput Assist Tomogr*. 1993; 17:536–546. [PubMed: 8331222]

Abbreviations List

ADME	absorption, distribution, metabolism, and excretion
ACh	acetylcholine
AChE	acetylcholinesterase
AD	Alzheimer's disease
CNS	central nervous system
ABV	aminobenzovesamicol
Anal	analysis
BBB	blood-brain-barrier
BBr₃	boron tribromide
<i>n</i>-BuLi	<i>n</i> -butyllithium
CDI	1,1'-carbonyldiimidazole
ChAT	choline acetyltransferase
CycA	Cyclosporine A
DMF	N,N-dimethylformamide
DMSO	dimethyl sulfoxide
(±)FBBV	(±)- <i>trans</i> -2-hydroxy-3-(4-(4-[¹⁸ F]fluorobenzoyl)piperidino)tetralin
IC₅₀	half maximum inhibitory constant
[¹²³I]IBVM	(-)-5-[¹²³ I]iodobenzovesamicol
NBS	N-bromosuccinimide
PD	Parkinson's Disease
PDD	Parkinson's disease associated with dementia
PET	positron emission tomography
P-gp	Permeability glycoprotein
σ₁ receptor	sigma-1 receptor
σ₂ receptor	sigma-2 receptor
SPECT	single photon emission computed tomography
TBDMSCI	<i>tert</i> -butyldimethylsilyl chloride
<i>t</i>-Boc	<i>tert</i> -butyloxycarbonyl
THF	tetrahydrofuran
TLC	thin layer chromatography
TFA	trifluoroacetic acid

TMSI	trimethylsilyl iodide
VAChT	vesicular acetylcholine transporter

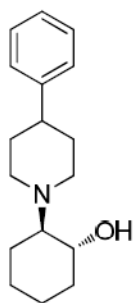
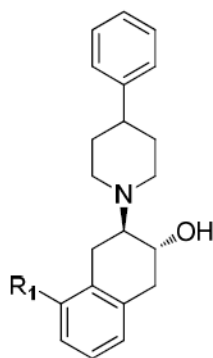
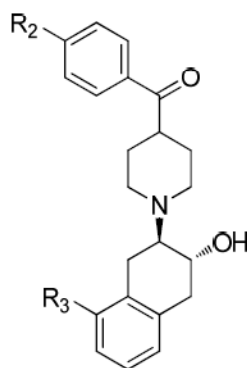
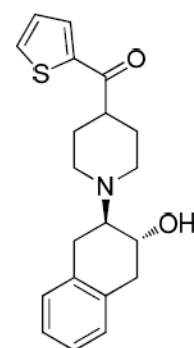
**Vesamicol****1, Benzovesamicol, R₁ = H****2, ABV, R₁ = NH₂****3, IBVM, R₁ = I****4, FEOBV, R₁ = OCH₂CH₂F****5, R₂ = H, R₃ = H****6, R₂ = NH₂, R₃ = H****7, R₂ = F, R₃ = H****8, R₂ = OCH₃, R₃ = H****9**

Figure 1.
Structures of VAcHT compounds

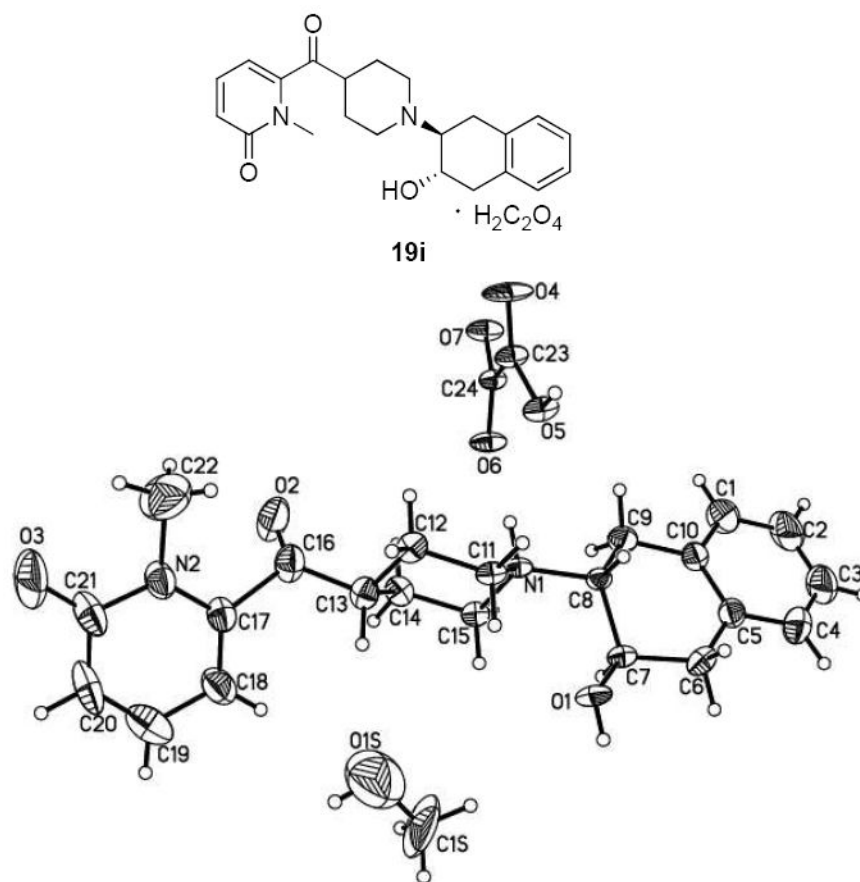


Figure 2.
Chemical structure and X-ray crystal structure of 19i.

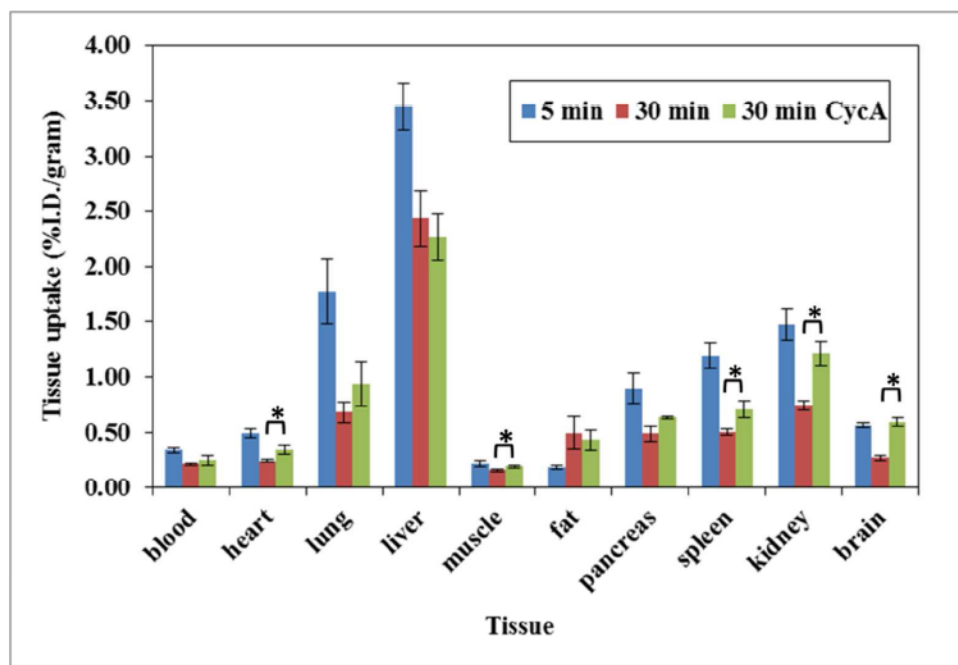


Figure 3.

The biodistribution of (-)- $[^{11}\text{C}]\mathbf{24b}$ in Sprague-Dawley Rats (185 – 205 gram). Control rats were euthanized at 5 and 30 min. Rats pretreated with at 25 mg/Kg of CycA 30 min prior to injection of the radiotracer. The star (*) in the figure are denoted that the %I.D./gram value from heart, muscle, spleen and brain were significantly different between non-CycA treated and CycA treated group ($n=4$, student t test, p -value <0.05).

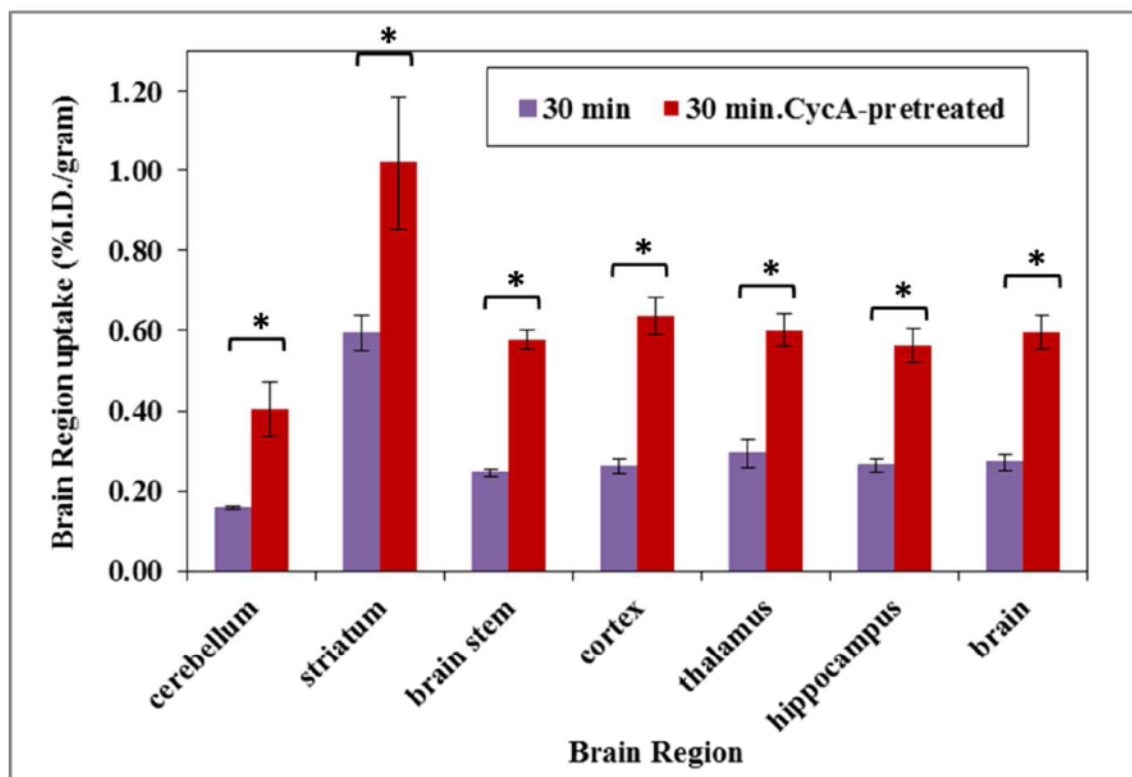


Figure 4.

The brain regional uptake of (-)-[¹¹C]24b in Sprague-Dawley rats at 30 min in control rats and rats pretreated with 25 mg/Kg of CycA 30 min prior to injection of the radiotracer. The star (*) in the figure are denoted that the % I.D./g value from all brain regions were significantly different between non-CycA treated and CycA treated group (n= 4, student t test, *p*-value <0.05).

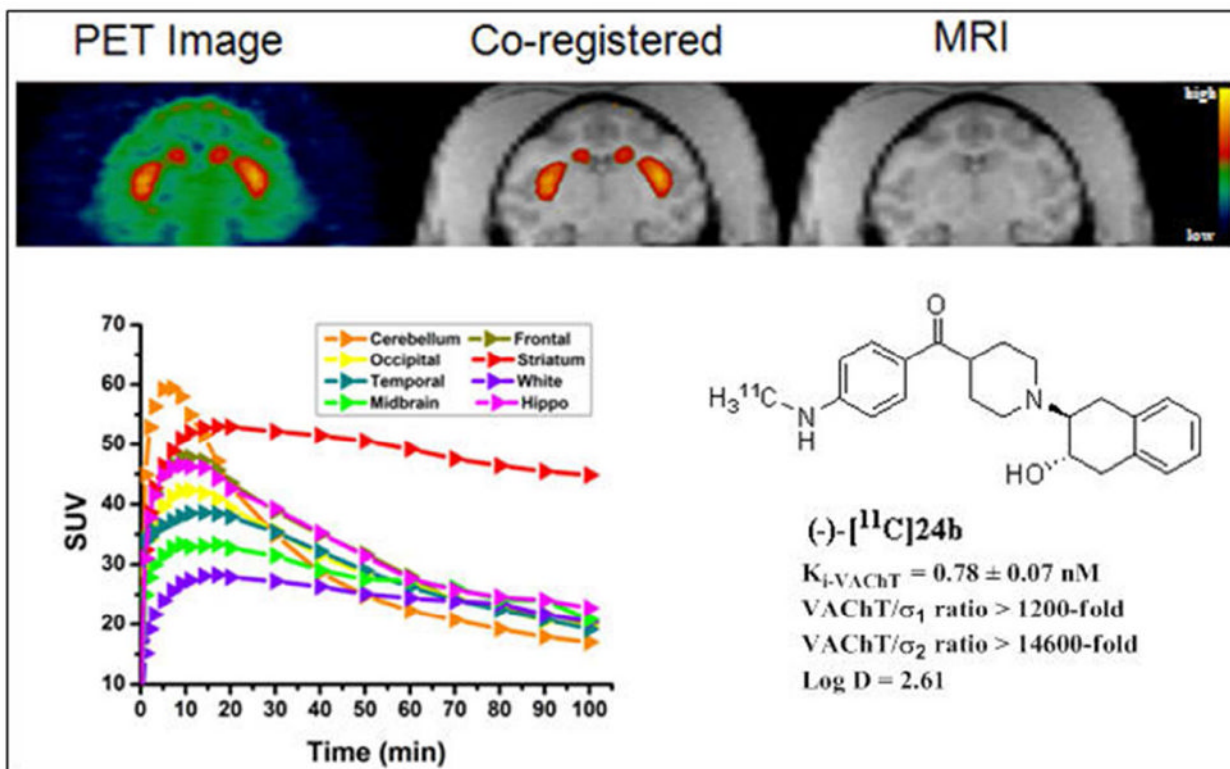
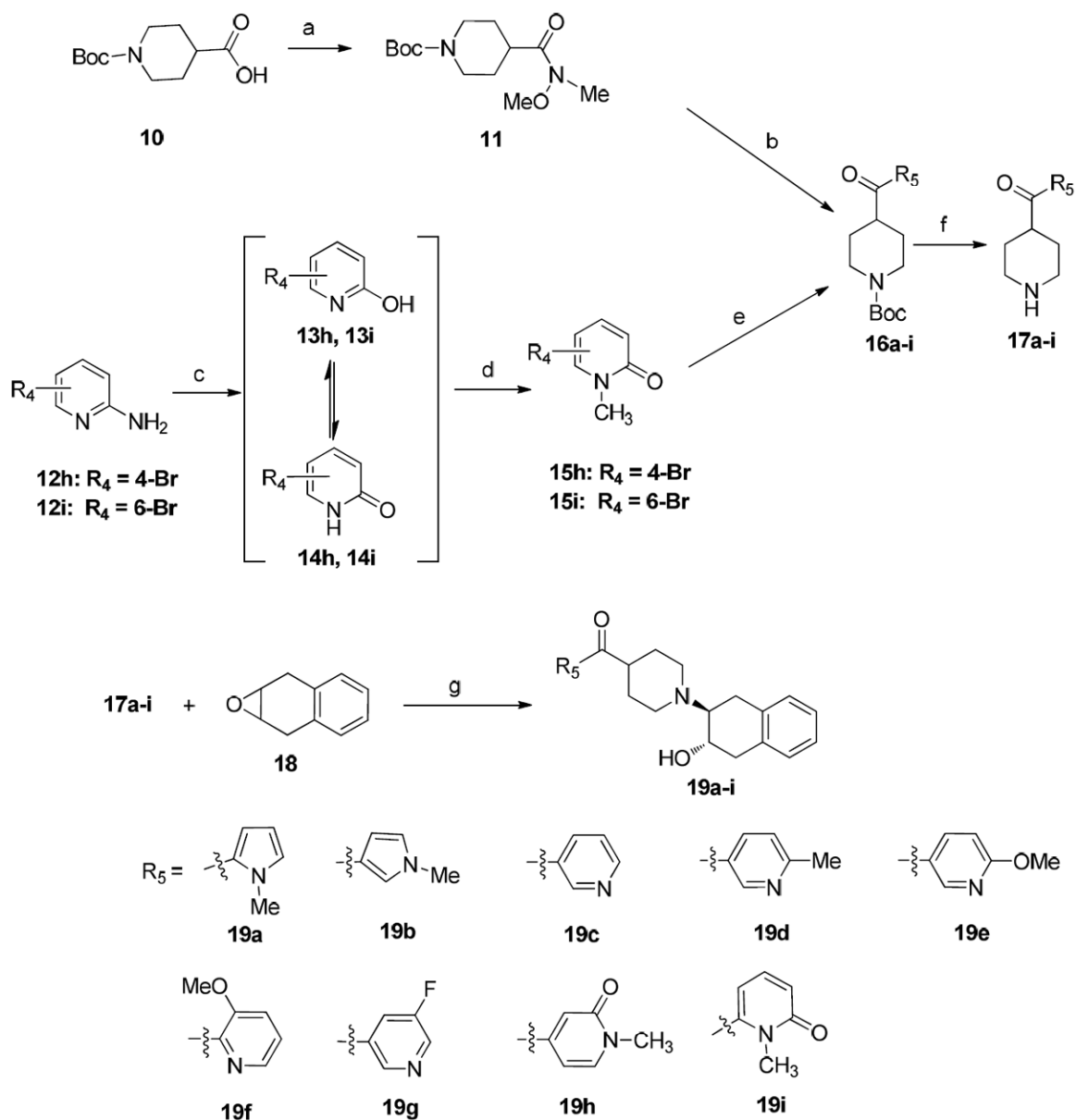
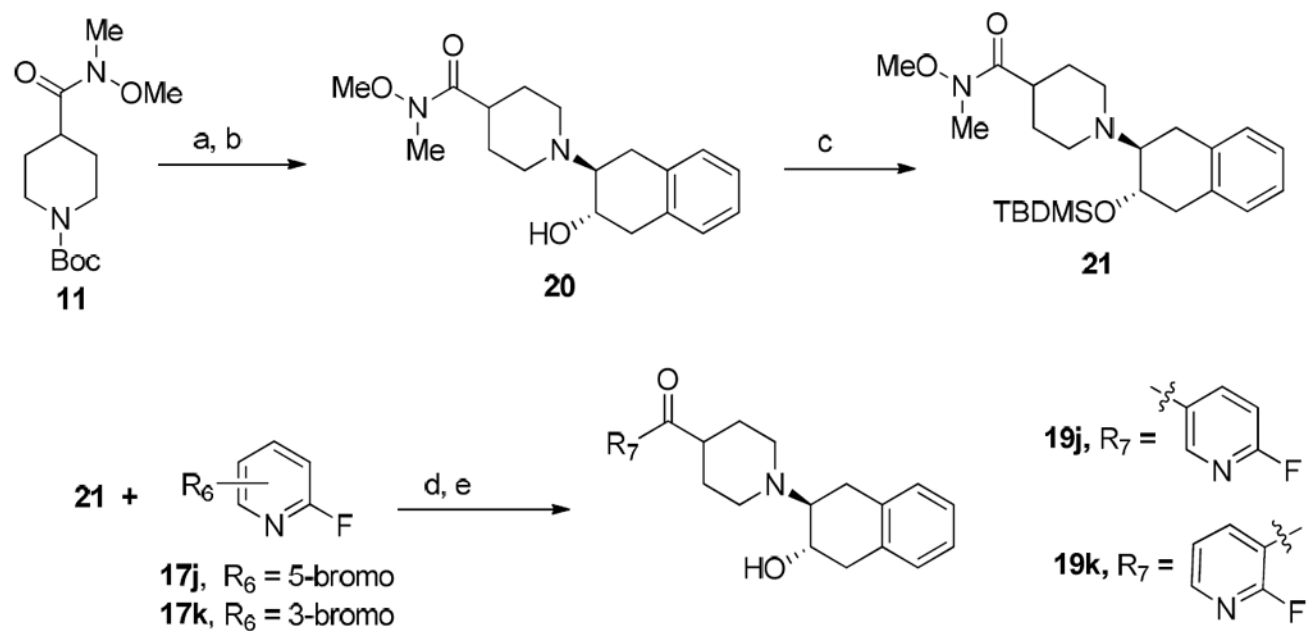


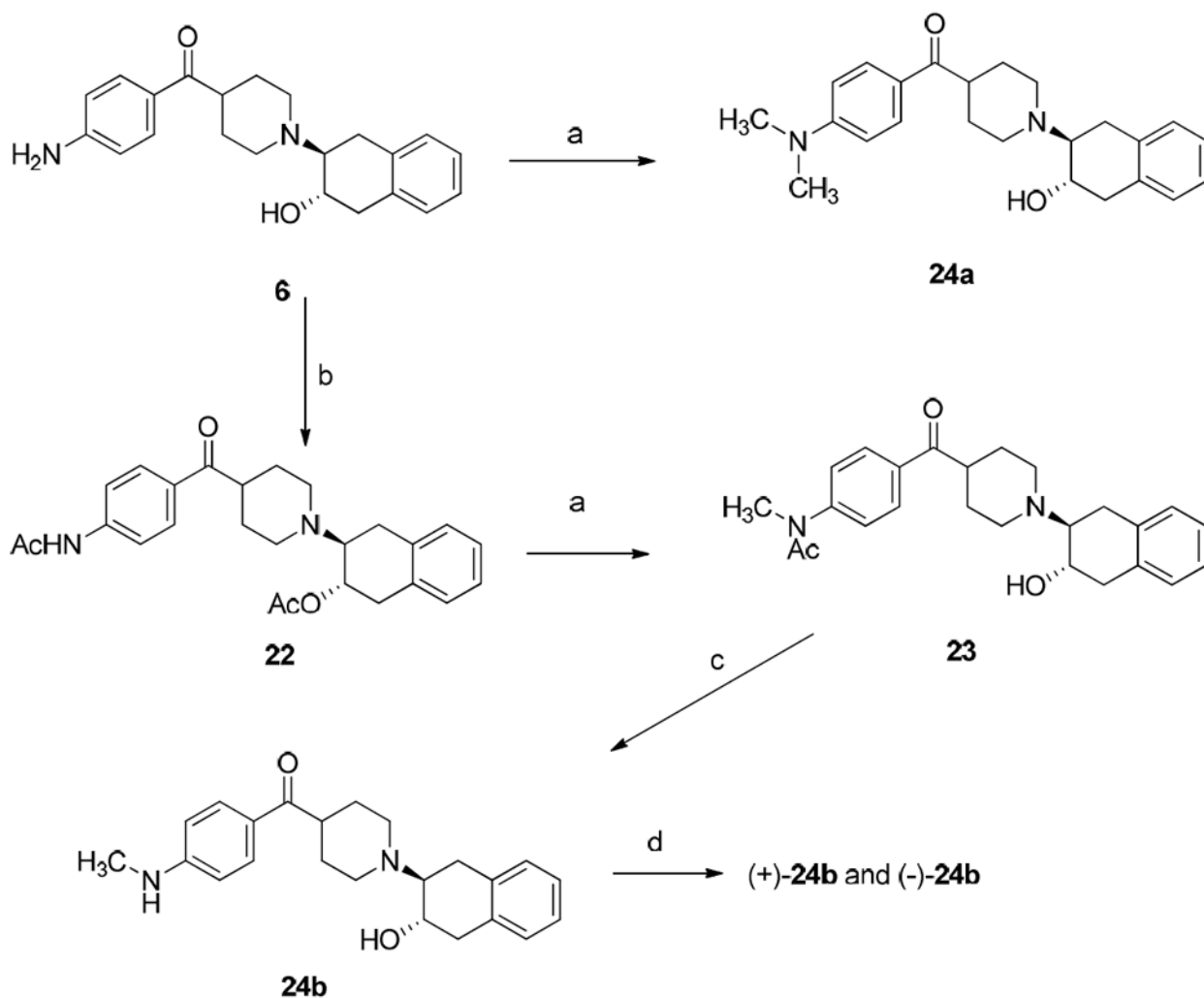
Figure 5. MicroPET imaging studies of (-)-[^{11}C]24b in cynomolgus monkey. MicroPET image (top left), co-registered image (top middle), MRI image (top right), time tissue-activity curve (left bottom).

**Scheme 1^a**^aReagents and conditions:

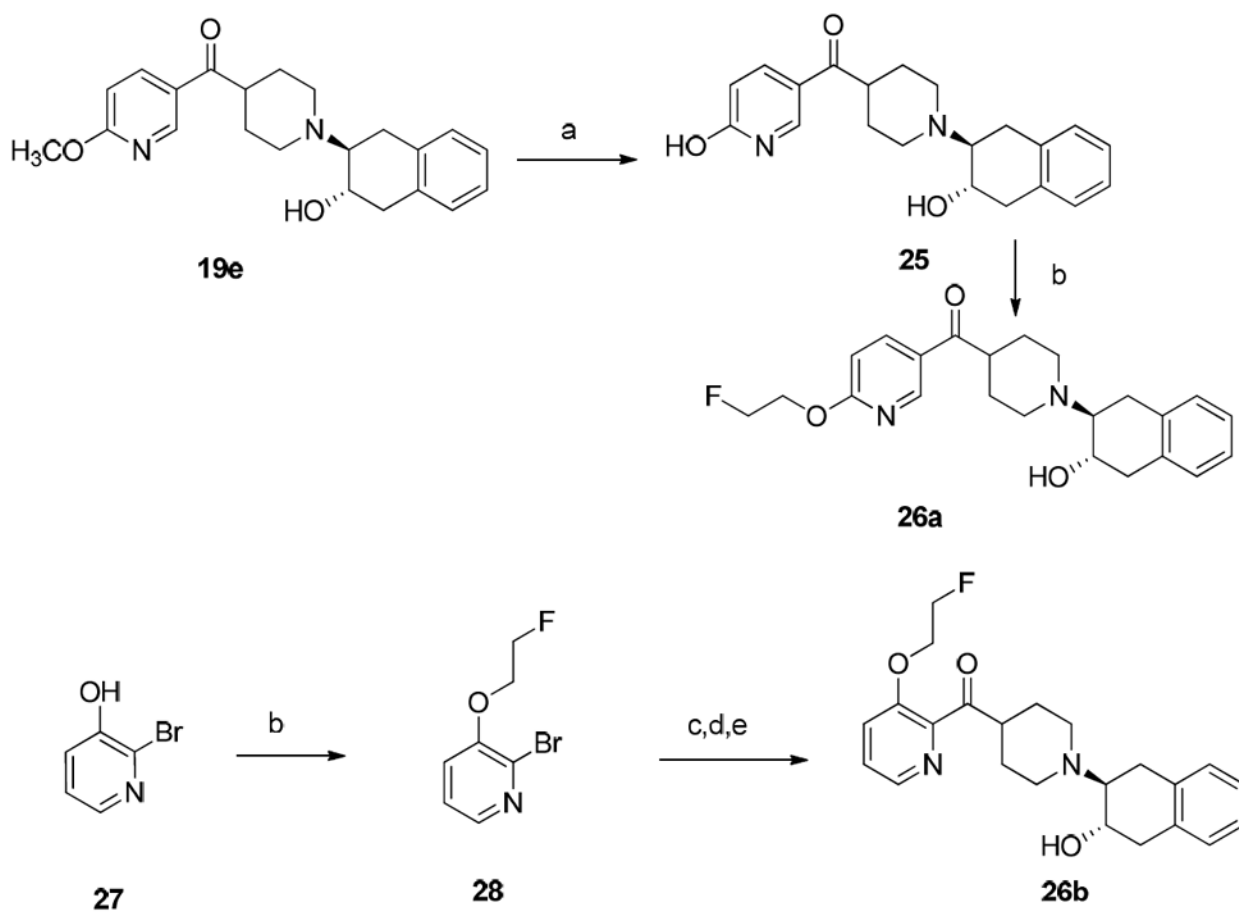
(a) CDI, N,O-Dimethylhydroxylamine hydrochloride, NEt_3 , CH_2Cl_2 , rt, overnight; (b) ArLi, THF; (c) $\text{H}_2\text{SO}_4/\text{NaNO}_2$, 0-5 °C, 2 h; (d) CH_3I , K_2CO_3 , acetone, 80 °C, 4 h; (e) **11**, BuLi, THF, -78 °C; (f) TFA, CH_2Cl_2 , rt, 4 h; (g) NEt_3 , EtOH, 75 °C, 36 h.

**Scheme 2^a**^aReagents and conditions:

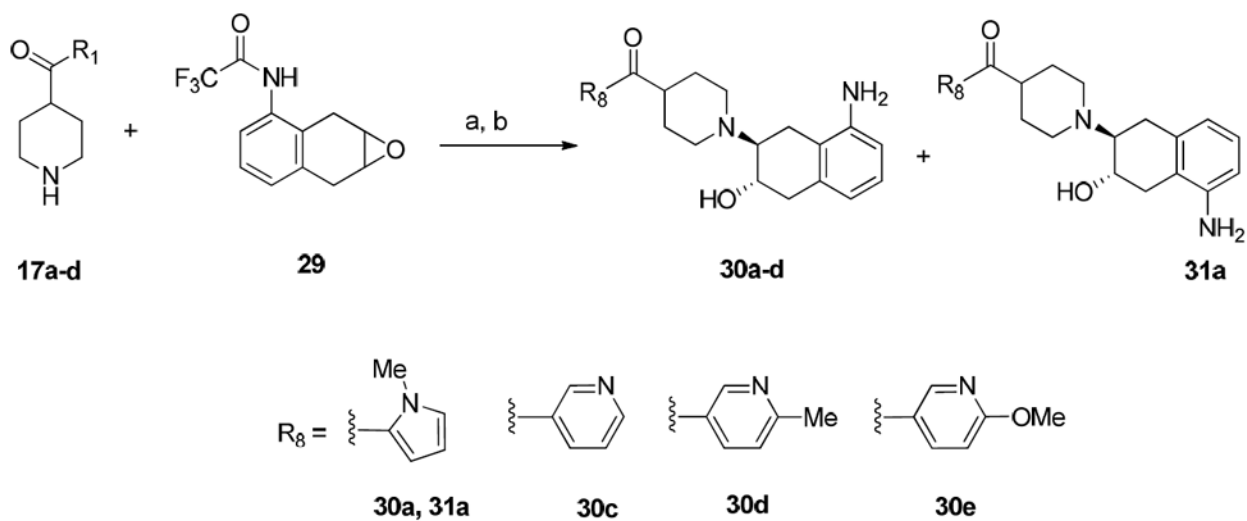
(a) TFA, CH_2Cl_2 , rt, 4 h; (b) 1,4-dihydronaphthalene oxide, NEt_3 , EtOH, 75 °C, 36 h; (c) TBDMSCl, imidazole, CH_2Cl_2 , rt, overnight; (d) *n*-BuLi, THF, -78 °C, 4h; (e) 12N HCl, THF, rt.

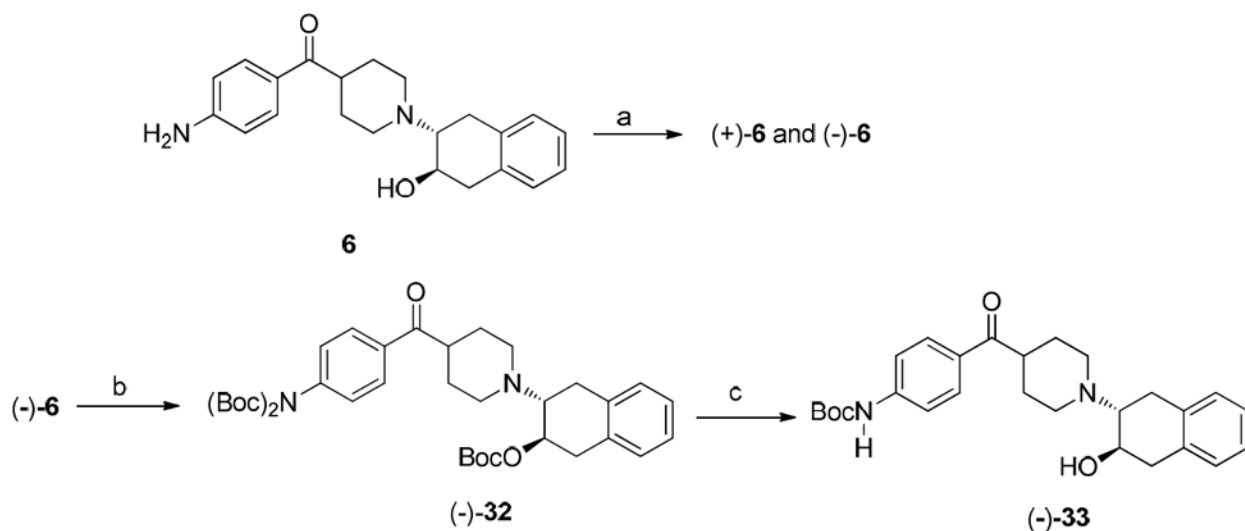
**Scheme 3^a**^aReagents and conditions:

(a) CH_3I , NaH, THF, rt, 0.5 h; (b) $(\text{CH}_3\text{CO})_2\text{O}$, Et_3N , CH_2Cl_2 , rt; (c) Concentrated HCl, ethylene glycol, refluxed; (d) Separation of enantiomers of **24b** on HPLC: column: Chiralcel OD; mobile phase: 35% isopropanol in hexane; flow rate: 4.0 mL/min; (+)-enantiomer at 15 min and (-)-enantiomer at 30 min;

**Scheme 4^a**^aReagents and conditions:

(a) BBr_3 or TMSI; (b) $\text{Br}(\text{CH}_2)_2\text{F}$, K_2CO_3 , DMF, rt, 72 h; (c) *tert*-butyl 4-(methoxy(methyl)carbamoyl) piperidine-1-carboxylate (**11**), BuLi, THF, -78°C ; (d) TFA, CH_2Cl_2 , rt, 4 h; (e) 1,4-dihydronaphthalene oxide, NEt_3 , EtOH, 75°C , 36 h.

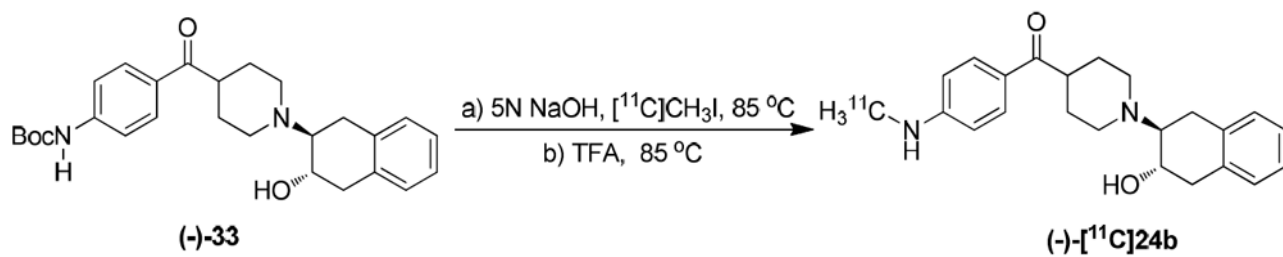
**Scheme 5^a**^aReagents and conditions:(a) NEt_3 , EtOH, 60 °C, 48 h; (b) 1N NaOH, EtOH, 60 °C, overnight.



Scheme 6^a Synthesis of the precursor (-)-33

^aReagents and conditions:

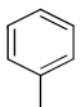
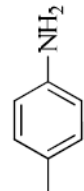
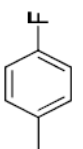
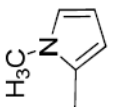
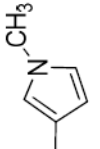
(a) Separation of enantiomers of **6** on HPLC: column: Chiralcel OD; mobile phase: 34% isopropanol in hexane; flow rate: 4.0 mL/min; (+)-enantiomer at 20.8 min and (-)-enantiomer at 33 min; (b) (Boc)₂O, DMAP, Et₃N, THF, rt., 1.5 h; (c) K₂CO₃, MeOH, reflux, overnight.

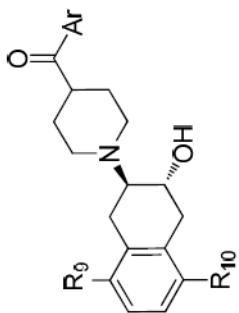


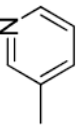
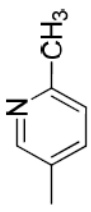
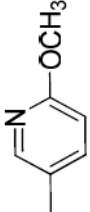
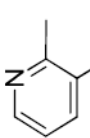
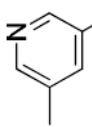
Scheme 7. Radiosynthesis of (-)-[¹¹C]24b

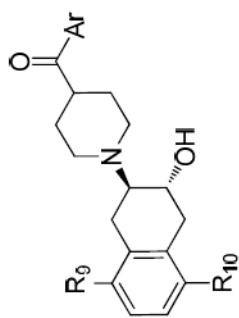
Table 1

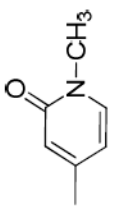
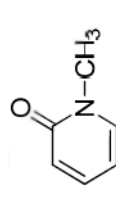
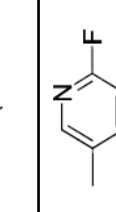
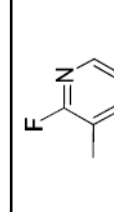
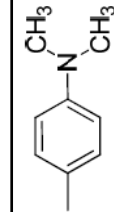
Binding affinities of new analogues for VACHT, α_1 receptor, and α_2 receptor

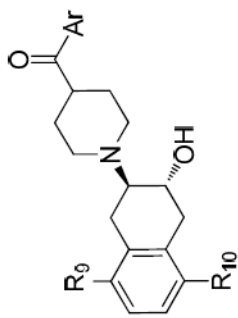
Compd	Ar	R ₉	R ₁₀	K _i (nM) ± SEM ^a			VACHT selectivity		ALog D ^e
				VACHT ^b	i ^c	z ^d	$\frac{K_{i\alpha 1}}{K_{i\text{VACHT}}}$	$\frac{K_{i\alpha 2}}{K_{i\text{VACHT}}}$	
5		H	H	4.30 ± 1.00	220 ± 17	320 ± 7	51	74	2.78
6		H	H	1.68 ± 0.14	NA	NA	NA	NA	1.56
7		H	H	2.70 ± 0.40	191 ± 58	251 ± 39	71	93	2.99
19a		H	H	18.4 ± 2.5	1300 ± 93	2550 ± 340	71	140	1.42
19b		H	H	26.6 ± 3.8	3040 ± 190	7710 ± 1060	110	290	1.84

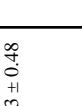

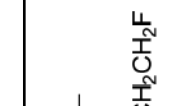
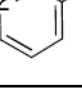
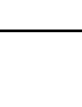


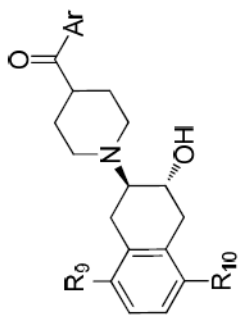
Compd	Ar	R ₉	R ₁₀	K _i (nM) ± SEM ^a			VACHT selectivity		ALog D ^c
				VACHT ^b	i ^c	i ^d	$\frac{K_{i\sigma 1}}{K_{i\text{VACHT}}}$	$\frac{K_{i\sigma 2}}{K_{i\text{VACHT}}}$	
19c		H	H	24.1 ± 2.8	12900 ± 3900	3030 ± 70	540	130	1.83
19d		H	H	27.9 ± 8.0	2120 ± 290	3770 ± 890	76	140	2.29
19e		H	H	8.36 ± 0.68	986 ± 160	2570 ± 140	120	310	2.64
19f		H	H	121 ± 29	21000 ± 3800	1560 ± 60	170	13	2.96
19g		H	H	10.1 ± 1.5	709 ± 79	1690 ± 60	70	170	1.99

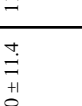

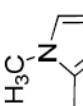
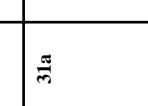



Compd	Ar	R ₉	R ₁₀	K _i (nM) ± SEM ^a		VACHT selectivity		ALog D ^c	
				VACHT ^b	i ^c	$\frac{K_{i\sigma 1}}{K_{iVACHT}}$	$\frac{K_{i\sigma 2}}{K_{iVACHT}}$		
19h		H	H	66.2 ± 10.2	3350 ± 50	2120 ± 250	51	32	0.60
19i		H	H	182 ± 65	2160 ± 180	3340 ± 130	12	18	0.64
19j		H	H	26.1 ± 2.4	682 ± 27	1750 ± 90	26	67	2.02
19k		H	H	12.7 ± 1.1	1300 ± 50	3530 ± 330	100	280	1.65
24a		H	H	0.93 ± 0.09	40.9 ± 8.2	4080 ± 100	44	4400	3.24



Compd	Ar	R ₉	R ₁₀	K _i (nM) ± SEM ^a			VAcHT selectivity		ALog D ^c
				VAcHT ^b	i ^c	2 ^d	$\frac{K_{i\sigma 1}}{K_{i\text{VAcHT}}}$	$\frac{K_{i\sigma 2}}{K_{i\text{VAcHT}}}$	
24b		H	H	3.03 ± 0.48	305 ± 22	6180 ± 540	100	2000	2.61
26a		H	H	38.0 ± 3.8	2120 ± 50	1860 ± 140	56	49	2.87
26b		H	H	76.4 ± 8.3	20000 ± 6800	303 ± 130	260	4.0	3.18
30a		NH ₂	H	38.7 ± 7.0	7660 ± 230	6990 ± 1480	200	180	0.53
30b		NH ₂	H	118 ± 24	20300 ± 8100	5080 ± 220	170	43	0.87



Compd	Ar	R ₉	R ₁₀	K _i (nM) ± SEM ^a			VACHT selectivity		ALog D ^c
				VACHT ^b	i ^c	2 ^d	$\frac{K_{i\sigma 1}}{K_{i\text{VACHT}}}$	$\frac{K_{i\sigma 2}}{K_{i\text{VACHT}}}$	
30c		NH ₂	H	48.0 ± 11.4	11400 ± 2000	27500 ± 6900	240	570	1.33
30d		NH ₂	H	23.3 ± 3.4	5680 ± 30	10800 ± 1300	120	220	1.66
31a		H	NH ₂	2310 ± 390	9240 ± 790	11400 ± 2500	4.0	4.9	0.53
(-)-24b		H	H	0.78 ± 0.07	992 ± 21	11443 ± 690	1271	14670	2.61
(+)-24b		H	H	19.0 ± 1.4	1170 ± 66	7765 ± 807	61.5	408	2.61

^aK_i values (mean ± SEM) were determined in at least three experiments for VACHT, 1 and 2 binding sites.

^bThe VACHT binding assay used expressed human VACHT.

^cThe ¹ binding assay used membrane preparations of guinea pig brain.

^dThe ² binding assay used homogenates of rat liver.

^eCalculated value at pH 7.4 by ACD/Labs, version 7.0 (Advanced Chemistry Development, Inc., Canada).